Preprint typeset in JHEP style - HYPER VERSION

UdeM-GPP-TH-09-186,TIFR/TH/09-43,UAB-FT/675

New-Physics Contributions to the Forward-Backward Asymmetry in $B \to K^* \mu^+ \mu^-$

Ashutosh Kumar Alok[a], Amol Dighe[b], Diptimoy Ghosh[b], David London[a], Joaquim Matias[c], Makiko Nagashima[a] and Alejandro Szynkman[a]

[a] *Physique des Particules, Université de Montréal, C.P. 6128, succ. centre-ville, Montréal, QC, Canada H3C 3J7*

[b] *Tata Institute of Fundamental Research, Homi Bhabha Road, Mumbai 400005, India*

[c] *Universitat Autonoma de Barcelona, Institut de Fisica d'Altes Energies, E-08193 Bellaterra, Barcelona, Spain*

E-mail: alok@lps.umontreal.ca, amol@theory.tifr.res.in, diptimoyghosh@theory.tifr.res.in, london@lps.umontreal.ca, matias@ifae.es, makiko@lps.umontreal.ca, szynkman@lps.umontreal.ca

Abstract: We study the forward-backward asymmetry ($A_{\rm FB}$) and the differential branching ratio (DBR) in $B \to K^* \mu^+ \mu^-$ in the presence of new physics (NP) with different Lorentz structures. We consider NP contributions from vector-axial vector (VA), scalar-pseudoscalar (SP), and tensor (T) operators, as well as their combinations. We calculate the effects of these new Lorentz structures in the low-q^2 and high-q^2 regions, and explain their features through analytic approximations. We find two mechanisms that can give a significant deviation from the standard-model predictions, in the direction indicated by the recent measurement of $A_{\rm FB}$ by the Belle experiment. They involve the addition of the following NP operators: (i) VA, or (ii) a combination of SP and T (slightly better than T alone). These two mechanisms can be distinguished through measurements of DBR in $B \to K^* \mu^+ \mu^-$ and $A_{\rm FB}$ in $B \to K \mu^+ \mu^-$.

Keywords: B Physics, Beyond Standard Model.

Contents

1. Introduction

To date, the standard model (SM) has been enormously successful in explaining the measurements of particle-physics experiments. However, recently some discrepancies with the predictions of the SM have been observed in B decays. Some examples are: (i) the values of the B^0_d-$\bar{B}^0_d$ mixing phase $\sin 2\beta$ obtained from different penguin-dominated $b \to s$ channels tend to be systematically smaller than that obtained from $B^0_d \to J/\psi K_S$ [1], (ii) in $B \to \pi K$ decays, it is difficult to account for all the experimental measurements within the SM [2], (iii) the measurement of the B^0_s-$\bar{B}^0_s$

mixing phase by the CDF and D0 collaborations deviates from the SM prediction [3], (iv) the isospin asymmetry between the neutral and the charged decay modes of the $\bar{B} \to \bar{K}^* l^+ l^-$ decay also differs from the SM [4]. Though the disagreements are only at the level of $\sim$ 2-3σ, and hence not statistically significant, they are intriguing since they all appear in $b \to s$ transitions.

Recently, one such discrepancy has been observed in the lepton forward-backward asymmetry ($A_{\rm FB}$) in the exclusive decay $\bar{B} \to \bar{K}^* \mu^+ \mu^-$ [5, 6]. This is especially interesting since it is a CP-conserving process, whereas most of the other discrepancies involve CP violation. The deviation from the SM can be seen in the differential $A_{\rm FB}$ as a function of the dilepton invariant mass q^2. In the high-q^2 region ($q^2 \geq 14.4$ GeV^2), the $A_{\rm FB}(q^2)$ measurements tend to be larger than the SM expectations, although both show similar trends. The anomaly is more striking at low q^2 (1 GeV$^2 \leq q^2 \leq 6$ GeV^2). In the first half of this region ($q^2 \leq 3$ GeV^2), the SM prediction is firmly negative [7], whereas the data favor positive values. Moreover, the SM predicts a zero crossing in $A_{\rm FB}(q^2)$ whose position is well-determined and free from hadronic uncertainties at leading order (LO) in α_s [8, 9]. The measurements, on the other hand, prefer positive values for $A_{\rm FB}(q^2)$ in the whole q^2-range, suggesting that there might not be a zero crossing. Indeed, Belle has claimed that this disagreement shows a clear hint of physics beyond the SM [10].

It is therefore quite natural to explore new-physics (NP) explanations of $A_{\rm FB}(q^2)$, and look for the effect of this NP on other observables in the same decay [11]. $\bar{B} \to \bar{K}^* \mu^+ \mu^-$ is described by the quark-level transition $b \to s \mu^+ \mu^-$. This is a flavor-changing neutral-current (FCNC) process, and is therefore expected to play an important role in the search for physics beyond the SM. There have already been a number of theoretical studies, both within the SM [12] and in specific NP scenarios [13], focusing on the branching fraction and $A_{\rm FB}$ of $\bar{B} \to \bar{K}^* \mu^+ \mu^-$. For example, Ref. [14] has pointed out that $A_{\rm FB}(q^2)$ is a sensitive probe of NP that affects the SM Wilson coefficients. Other observables based on the K^* spin amplitudes of this decay are at present under active theoretical and experimental analysis [15, 16, 17]. Finally, more challenging observables, such as the polarized lepton forward-backward asymmetry [18], have also been considered, though the measurement of this quantity is still lacking.

In the coming years, the LHCb experiment [19] will collect around 6.4k events in the full range of q^2 for an integrated luminosity of 2 fb^{-1} (a nominal one-year data taking). This would allow the extraction of the SM zero (if it is there) of $A_{\rm FB}$ with a precision of ± 0.5 GeV^2. Indeed a dataset of 100 pb^{-1} would already improve the world precision obtained by Babar, Belle and CDF. These measurements would also permit many of the additional tests for NP mentioned above.

The decays $\bar{B} \to X_s \mu^+ \mu^-$ and $\bar{B} \to \bar{K} \mu^+ \mu^-$ are also described by $b \to s \mu^+ \mu^-$, and hence the same new physics would be expected to affect their measurements. The branching ratios of these decays offer significant constraints on NP contribu-

tions from all Lorentz structures. The possibility of a large $A_{\rm FB}$ in $\bar{B} \to \bar{K}\mu^+\mu^-$ was considered in Ref. [20], where a general analysis, allowing for all possible NP effects, was performed. This included vector-axial vector (VA), scalar-pseudoscalar (SP), and tensor (T) operators. It was shown that $A_{\rm FB}(q^2)$ in this decay cannot be enhanced significantly with new VA operators, while T operators can increase $A_{\rm FB}(q^2)$ efficiently, especially when combined with the SP new physics.

In this paper, we apply the method of Ref. [20] to the decay $\bar{B} \to \bar{K}^*\mu^+\,\mu^-$. That is, we perform a general analysis of NP effects without restricting ourselves to a specific model. Our aim here is not to obtain precise predictions, but rather to obtain an understanding of how the NP affects the observables, and to establish which Lorentz structure(s) can accommodate the observed $A_{\rm FB}(q^2)$ anomaly. The impact of NP in $A_{\rm FB}(q^2)$ may be partly washed out by integrating over q^2, so we study the differential $A_{\rm FB}(q^2)$ in the entire q^2 region.

We find that, after taking into account the constraints from relevant measurements, there are two NP Lorentz structures that can give predictions closer to the low-q^2 $A_{\rm FB}$ data than the SM. The first is the case in which one adds new VA operators. Here, the values of $A_{\rm FB}(q^2)$ can be always positive, and hence there is no zero crossing. In the second, NP T operators are present, which can shift the crossing point to much lower q^2 values. The addition of SP operators to the T operators allows the results to be somewhat closer to the data. We also point out the effects of viable NP scenarios on the differential branching fraction dB/dq^2.

In section 2, we review the decay $\bar{B} \to \bar{K}^*\mu^+\,\mu^-$ within the SM. We introduce new physics in section 3 by adding all possible NP operators to the effective Hamiltonian. We also calculate the constraints on the coefficients of these operators, and present the theoretical expressions for $A_{\rm FB}(q^2)$ and dB/dq^2 for $\bar{B} \to \bar{K}^*\mu^+\,\mu^-$. Section 4 contains our numerical results for $A_{\rm FB}(q^2)$ and dB/dq^2 with the addition of specific viable NP operators. In section 5, we summarize our findings and discuss their implications. Some of the more complicated algebraic expressions can be found in the appendix A.

2. $\bar{B} \to \bar{K}^*\mu^+\,\mu^-$: Standard Model

Within the SM, the effective Hamiltonian for the quark-level transition $b \to s\mu^+\mu^-$ is

$$\begin{aligned}\mathcal{H}_{\rm eff}^{SM} &= -\frac{4G_F}{\sqrt{2}}\,V_{ts}^*V_{tb}\Big\{\sum_{i=1}^{6}C_i(\mu)\mathcal{O}_i(\mu) + C_7\,\frac{e}{16\pi^2}\,(\bar{s}\sigma_{\mu\nu}(m_sP_L + m_bP_R)b)\,F^{\mu\nu} \\ &\quad + C_9\,\frac{\alpha_{em}}{4\pi}\,(\bar{s}\gamma^\mu P_L b)\,\bar{\mu}\gamma_\mu\mu + C_{10}\,\frac{\alpha_{em}}{4\pi}\,(\bar{s}\gamma^\mu P_L b)\,\bar{\mu}\gamma_\mu\gamma_5\mu\Big\}\,, \qquad (2.1)\end{aligned}$$

where $P_{L,R} = (1 \mp \gamma_5)/2$. The operators $\mathcal{O}_i$ $(i = 1,..6)$ correspond to the P_i in Ref. [21]. The SM Wilson coefficients take the following values at the scale $\mu = 4.8$

GeV in next-to-next-to-leading order [7]:

$$C_7^{\rm eff} = -0.304 \quad , \quad C_9^{\rm eff} = 4.211 + Y(q^2) \quad , \quad C_{10} = -4.103 \; , \tag{2.2}$$

where $C_7^{\rm eff} = C_7 - C_3/3 - 4C_4/9 - 20C_5/3 - 80C_6/9$, q^μ is the sum of the 4-momenta of the μ^+ and μ^-, and the function $Y(q^2)$ is given by [9]

$$\begin{aligned} Y(q^2) = & \, h(q^2, m_c) \left(\frac{4}{3} C_1 + C_2 + 6\, C_3 + 60\, C_5 \right) \\ & - \frac{1}{2} h(q^2, m_b) \left(7 C_3 + \frac{4}{3} C_4 + \, 76 C_5 + \frac{64}{3} C_6 \right) \\ & - \frac{1}{2} h(q^2, 0) \left(C_3 + \frac{4}{3} C_4 + 16\, C_5 + \frac{64}{3} C_6 \right) + \frac{4}{3} C_3 + \frac{64}{9} C_5 + \frac{64}{27} C_6 \; . \end{aligned} \tag{2.3}$$

Here

$$h(s, m_q) = -\frac{4}{9} \left(\ln \frac{m_q^2}{\mu^2} - \frac{2}{3} - x \right) - \frac{4}{9} (2+x) \sqrt{|x-1|} \begin{cases} \arctan \dfrac{1}{\sqrt{x-1}} & x > 1 \\ \ln \dfrac{1+\sqrt{1-x}}{\sqrt{x}} - \dfrac{i\pi}{2} & x \le 1 \end{cases} \tag{2.4}$$

with $x = 4m_q^2/q^2$. A tiny weak phase has been neglected.

The decay amplitude for $\bar{B}(p_1) \to \bar{K}^*(p_2, \epsilon)\, \mu^+(p_+)\, \mu^-(p_-)$ is

$$\begin{aligned} M(\bar{B} \to \bar{K}^* \mu^+ \mu^-) \;\; = \;\; & \frac{\alpha G_F}{2\sqrt{2}\pi} V_{ts}^* V_{tb} \times \\ & \Big[\langle \bar{K}^*(p_2, \epsilon)\, | \bar{s} \gamma^\mu (1-\gamma_5) b |\, \bar{B}(p_1) \rangle \Big\{ C_9^{\rm eff}\, \bar{u}(p_-) \gamma_\mu v(p_+) + C_{10}\, \bar{u}(p_-) \gamma_\mu \gamma_5 v(p_+) \Big\} \\ & - 2\, \frac{C_7^{\rm eff}}{q^2}\, m_b \langle \bar{K}^*(p_2, \epsilon) | \bar{s} i \sigma_{\mu\nu} q^\nu (1+\gamma_5) b | \bar{B}(p_1) \rangle\, \bar{u}(p_-) \gamma^\mu v(p_+) \Big] \; , \end{aligned} \tag{2.5}$$

where we have neglected the strange-quark mass m_s. The expressions for the matrix elements as a function of form factors are given in Ref. [22], and are reproduced in Appendix A for the sake of completeness.

The double differential decay rate is given by

$$\frac{d^2\Gamma}{dq^2 d\cos\theta} = \frac{1}{2m_B} \frac{2v\sqrt{\lambda}}{(8\pi)^3} |M|^2 \; , \tag{2.6}$$

where $v \equiv \sqrt{1 - 4m_l^2/q^2}$. Here $\lambda \equiv 1 + \hat{r}^2 + z^2 - 2(\hat{r} + z) - 2\hat{r}z$, with $\hat{r} \equiv m_{K^*}^2/m_B^2$ and $z \equiv q^2/m_B^2$. The forward-backward asymmetry for the muons is defined by

$$A_{\rm FB}(q^2) = \frac{\displaystyle\int_0^1 d\cos\theta \frac{d^2\Gamma}{dq^2 d\cos\theta} - \int_{-1}^0 d\cos\theta \frac{d^2\Gamma}{dq^2 d\cos\theta}}{\displaystyle\int_0^1 d\cos\theta \frac{d^2\Gamma}{dq^2 d\cos\theta} + \int_{-1}^0 d\cos\theta \frac{d^2\Gamma}{dq^2 d\cos\theta}} \; , \tag{2.7}$$

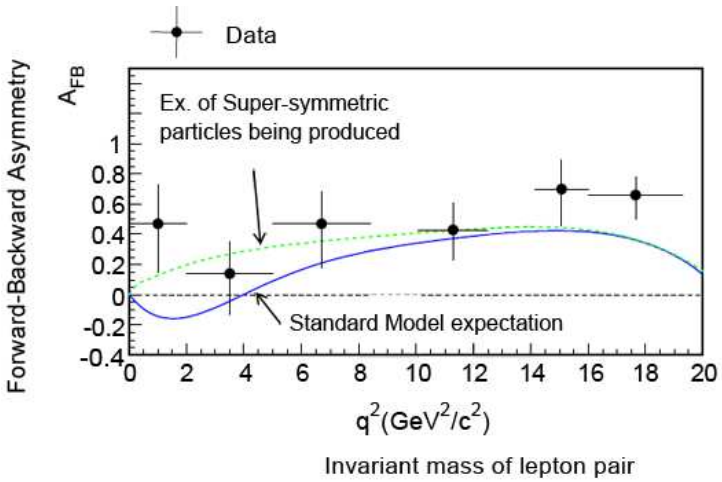

Figure 1: The SM prediction for $A_{\rm FB}(q^2)$ in $\bar{B} \to \bar{K}^* \mu^+ \mu^-$ and the experimental measurements from Belle. This figure is taken from Ref. [10].

where θ is the angle between the momenta of the B and the μ^+ in the dimuon center-of-mass frame.

In Fig. 1, we show the SM prediction for $A_{\rm FB}(q^2)$, along with the experimental measurements from Belle. From this figure, we see that the discrepancy with the SM is the strongest in the low-q^2 region, where the SM predicts negative values of $A_{\rm FB}(q^2)$, as well as a zero crossing. The zero of $A_{\rm FB}(q^2)$ is particularly clean, because at this point the form-factor dependence cancels at LO, and a relation between the short-distance coefficients is predicted [23]:

$$\mathrm{Re}(C_9^{\rm eff}(q_0^2)) = -\frac{2 m_B m_b}{q_0^2}\, C_7^{\rm eff} \ , \tag{2.8}$$

where q_0^2 is the point where $A_{\rm FB}(q_0^2) = 0$. Next-to-leading-order (NLO) contributions shift the position of this zero to a higher value: $q_0^2 = 3.90 \pm 0.12\,\mathrm{GeV}^2$ [7]. A substantial deviation from this zero crossing point would thus be a robust signal for new physics. This can occur if the NP affects $C_7^{\rm eff}$ and/or $C_9^{\rm eff}$, or if it changes the above relation itself, such as by introducing new Wilson coefficients. The present experimental data point towards positive values of $A_{\rm FB}(q^2)$ in the entire q^2 region, thus favoring a non-crossing solution. In the following sections, we therefore look for sources of NP which can give rise to this feature.

3. $\bar{B} \to \bar{K}^* \mu^+ \mu^-$: New-Physics Lorentz Structures

3.1 New-physics operators

We now add new physics to the effective Hamiltonian for $b \to s\mu^+\mu^-$, so that it becomes

$$\mathcal{H}_{\rm eff}(b \to s\mu^+\mu^-) = \mathcal{H}_{\rm eff}^{SM} + \mathcal{H}_{\rm eff}^{VA} + \mathcal{H}_{\rm eff}^{SP} + \mathcal{H}_{\rm eff}^{T} \ , \tag{3.1}$$

where $\mathcal{H}_{\rm eff}^{SM}$ is given by Eq. (2.1), while

$$\begin{aligned}
\mathcal{H}_{\rm eff}^{VA} &= -\frac{\alpha G_F}{\sqrt{2}\pi}\, V_{ts}^* V_{tb} \Big\{ R_V\, \bar{s}\gamma^\mu P_L b\, \bar{\mu}\gamma_\mu \mu + R_A\, \bar{s}\gamma^\mu P_L b\, \bar{\mu}\gamma_\mu\gamma_5\mu \\
&\qquad + R'_V\, \bar{s}\gamma^\mu P_R b\, \bar{\mu}\gamma_\mu \mu + R'_A\, \bar{s}\gamma^\mu P_R b\, \bar{\mu}\gamma_\mu\gamma_5\mu \Big\}\,, \qquad (3.2) \\
\mathcal{H}_{\rm eff}^{SP} &= -\frac{\alpha G_F}{\sqrt{2}\pi}\, V_{ts}^* V_{tb} \Big\{ R_S\, \bar{s}P_R b\, \bar{\mu}\mu + R_P\, \bar{s}P_R b\, \bar{\mu}\gamma_5\mu \\
&\qquad + R'_S\, \bar{s}P_L b\, \bar{\mu}\mu + R'_P\, \bar{s}P_L b\, \bar{\mu}\gamma_5\mu \Big\}\,, \qquad (3.3) \\
\mathcal{H}_{\rm eff}^{T} &= -\frac{\alpha G_F}{\sqrt{2}\pi}\, V_{ts}^* V_{tb} \Big\{ C_T\, \bar{s}\sigma_{\mu\nu} b\, \bar{\mu}\sigma^{\mu\nu}\mu + iC_{TE}\, \bar{s}\sigma_{\mu\nu} b\, \bar{\mu}\sigma_{\alpha\beta}\mu\, \epsilon^{\mu\nu\alpha\beta} \Big\} \qquad (3.4)
\end{aligned}$$

are the new contributions. Here, $R_V, R_A, R'_V, R'_A, R_S, R_P, R'_S, R'_P, C_T$ and C_{TE} are the NP couplings. For simplicity, in our numerical analysis of the forward-backward asymmetry and the differential branching ratio, these couplings are taken to be real. However, for completeness, the expressions allow for a complex-coupling analysis.

As was done in the SM case, one can turn the expression of the effective Hamiltonian for $b \to s\mu^+\mu^-$ into a decay amplitude for $\bar{B}(p_1) \to \bar{K}^*(p_2)\,\mu^+(p_+)\,\mu^-(p_-)$. This amplitude is

$$\begin{aligned}
M(\bar{B} \to \bar{K}^* \mu^+ \mu^-) &= \frac{\alpha G_F}{2\sqrt{2}\pi}\, V_{ts}^* V_{tb} \times \\
&\Big[\langle \bar{K}^*(p_2,\epsilon)|\bar{s}\gamma^\mu(1-\gamma_5)b|\bar{B}(p_1)\rangle \Big\{ (C_9^{\rm eff} + R_V)\, \bar{u}(p_-)\gamma_\mu v(p_+) \\
&\qquad + (C_{10} + R_A)\, \bar{u}(p_-)\gamma_\mu\gamma_5 v(p_+) \Big\} \\
&\quad + \langle \bar{K}^*(p_2,\epsilon)|\bar{s}\gamma^\mu(1+\gamma_5)b|\bar{B}(p_1)\rangle \Big\{ R'_V\, \bar{u}(p_-)\gamma_\mu v(p_+) + R'_A\, \bar{u}(p_-)\gamma_\mu\gamma_5 v(p_+) \Big\} \\
&\quad - 2\,\frac{C_7^{\rm eff}}{q^2}\, m_b\, \langle \bar{K}^*(p_2,\epsilon)|\bar{s} i\sigma_{\mu\nu} q^\nu (1+\gamma_5) b|\bar{B}(p_1)\rangle\, \bar{u}(p_-)\gamma^\mu v(p_+) \\
&\quad + \langle \bar{K}^*(p_2,\epsilon)|\bar{s}(1+\gamma_5)b|\bar{B}(p_1)\rangle\, \{ R_S\, \bar{u}(p_-)v(p_+) + R_P\, \bar{u}(p_-)\gamma_5 v(p_+) \} \\
&\quad + \langle \bar{K}^*(p_2,\epsilon)|\bar{s}(1-\gamma_5)b|\bar{B}(p_1)\rangle\, \{ R'_S\, \bar{u}(p_-)v(p_+) + R'_P\, \bar{u}(p_-)\gamma_5 v(p_+) \} \\
&\quad + 2\, C_T\, \langle \bar{K}^*(p_2,\epsilon)|\bar{s}\sigma_{\mu\nu} b|\bar{B}(p_1)\rangle\, \bar{u}(p_-)\sigma^{\mu\nu} v(p_+) \\
&\quad + 2i\, C_{TE}\, \epsilon^{\mu\nu\alpha\beta} \langle \bar{K}^*(p_2,\epsilon)|\bar{s}\sigma_{\mu\nu} b|\bar{B}(p_1)\rangle\, \bar{u}(p_-)\sigma_{\alpha\beta} v(p_+) \Big]\,, \qquad (3.5)
\end{aligned}$$

where the expressions for the matrix elements [22] are reproduced in appendix A. Note that the matrix elements are functions of 7 form factors: $A_{0,1,2}(q^2)$, $V(q^2)$, $T_{1,2,3}(q^2)$.

3.2 Constraints on the new-physics couplings

The constraints on the NP couplings in $b \to s\,\mu^+\,\mu^-$ are obtained mainly from the related decays $\bar{B} \to X_s\,\mu^+\,\mu^-$ and $\bar{B}_s^0 \to \mu^+\,\mu^-$. Due to the large hadronic

uncertainties, the exclusive decays $\bar{B} \to (\bar{K}, \bar{K}^*)\,\mu^+\,\mu^-$ provide weaker constraints than the inclusive decay $\bar{B} \to X_s\,\mu^+\,\mu^-$.

Neglecting the muon and strange-quark masses, the branching ratio of $\bar{B} \to X_s\,\mu^+\,\mu^-$ is given by

$$\begin{aligned} B(\bar{B} \to X_s\,\mu^+\,\mu^-) &= B_{SM} + B_{VA}\left[|R_V|^2 + |R_A|^2 + |R'_V|^2 + |R'_A|^2\right] \\ &\quad + B_{SM\text{-}VA}\mathrm{Re}\left[R_V^* C_9^{\mathrm{eff}} + R_A^* C_{10}\right] + B'_{SM\text{-}VA}\mathrm{Re}(R_V^* C_7^{\mathrm{eff}}) \\ &\quad + B_{SP}\left[|R_S|^2 + |R_P|^2 + |R'_S|^2 + |R'_P|^2\right] + B_T\left[|C_T|^2 + 4|C_{TE}|^2\right] , \end{aligned} \tag{3.6}$$

where

$$\begin{aligned} B_{SM} &= B_0 \int_{z_{\min}}^{z_{\max}} dz\,(1-z)\left[\frac{16}{z}\left\{1 - z^2 + \frac{(1-z)^2}{3}\right\}(C_7^{\mathrm{eff}})^2\right. \\ &\quad \left. + 4\left\{1 - z^2 - \frac{(1-z)^2}{3}\right\}\left[|C_9^{\mathrm{eff}}|^2 + C_{10}^2\right] + 32\,(1-z)\,C_7^{\mathrm{eff}}\,\mathrm{Re}(C_9^{\mathrm{eff}})\right] , \\ B_{VA} &= 4\,B_0 \int_{z_{\min}}^{z_{\max}} dz\,(1-z)\left\{1 - z^2 - \frac{(1-z)^2}{3}\right\} , \\ B_{SM\text{-}VA} &= 2\,B_{VA} , \qquad B_T \;=\; 16\,B_{VA} , \\ B'_{SM\text{-}VA} &= 32\,B_0 \int_{z_{\min}}^{z_{\max}} dz\,(1-z)^2 , \qquad B_{SP} \;=\; 4\,B_0 \int_{z_{\min}}^{z_{\max}} dz\,z\,(1-z)^2 , \end{aligned} \tag{3.7}$$

with $z \equiv q^2/m_b^2$. The normalization constant B_0 is

$$B_0 = \frac{3\alpha^2\,B(\bar{B} \to X_c e\bar{\nu})}{32\pi^2\,f(\hat{m}_c)\,\kappa(\hat{m}_c)}\frac{|V_{tb}^* V_{ts}|^2}{|V_{cb}^*|^2} , \tag{3.8}$$

where $\hat{m}_c \equiv m_c/m_b$. Here $f(\hat{m}_c)$ is the phase-space factor in $B(\bar{B} \to X_c e\bar{\nu})$ [24]:

$$f(\hat{m}_c) = 1 - 8\hat{m}_c^2 + 8\hat{m}_c^6 - \hat{m}_c^8 - 24\hat{m}_c^4 \ln \hat{m}_c , \tag{3.9}$$

and $\kappa(\hat{m}_c)$ is the 1-loop QCD correction factor [24]

$$\kappa(\hat{m}_c) = 1 - \frac{2\alpha_s(m_b)}{3\pi}\left[\left(\pi^2 - \frac{31}{4}\right)(1-\hat{m}_c)^2 + \frac{3}{2}\right] . \tag{3.10}$$

The branching ratio of $\bar{B} \to X_s\,\mu^+\,\mu^-$ has been measured by both Belle [25] and BaBar [26]. In the low-q^2 ($1\ \mathrm{GeV}^2 \le q^2 \le 6\ \mathrm{GeV}^2$) and high-$q^2$ ($14.4\ \mathrm{GeV}^2 \le q^2 \le 25\ \mathrm{GeV}^2$) regions, the measurements are

$$B(\bar{B} \to X_s\,\mu^+\,\mu^-)_{\text{low } q^2} = \begin{cases} \left(1.49 \pm 0.50^{+0.41}_{-0.32}\right) \times 10^{-6} , & \text{(Belle)} , \\ (1.8 \pm 0.7 \pm 0.5) \times 10^{-6} , & \text{(BaBar)} , \\ (1.60 \pm 0.50) \times 10^{-6} , & \text{(Average)} . \end{cases} \tag{3.11}$$

$$B(\bar{B} \to X_s\,\mu^+\,\mu^-)_{\text{high } q^2} = \begin{cases} \left(0.42 \pm 0.12^{+0.06}_{-0.07}\right) \times 10^{-6} , & \text{(Belle)} , \\ \left(0.50 \pm 0.25^{+0.08}_{-0.07}\right) \times 10^{-6} , & \text{(BaBar)} , \\ (0.44 \pm 0.12) \times 10^{-6} , & \text{(Average)} . \end{cases} \tag{3.12}$$

The SM predictions for $B(\bar{B} \to X_s\,\mu^+\,\mu^-)$ in the low- and high-q^2 regions are $(1.59 \pm 0.11) \times 10^{-6}$ and $(0.24 \pm 0.07) \times 10^{-6}$, respectively [27].

The branching ratio of $\bar{B}_s^0 \to \mu^+\,\mu^-$ in the presence of the NP operators is

$$B(\bar{B}_s \to \mu^+\,\mu^-) = \frac{G_F^2 \alpha^2 m_{B_s}^5 f_{B_s}^2 \tau_{B_s}}{64\pi^3} |V_{tb} V_{ts}^*|^2 \sqrt{1 - \frac{4m_\mu^2}{m_{B_s}^2}}$$
$$\times \left\{ \left(1 - \frac{4m_\mu^2}{m_{B_s}^2}\right) \left| \frac{R_S - R_S'}{m_b + m_s} \right|^2 + \left| \frac{R_P - R_P'}{m_b + m_s} + \frac{2m_\mu}{m_{B_s}^2} (C_{10} + R_A - R_A') \right|^2 \right\}. \quad (3.13)$$

The SM prediction for $B(\bar{B}_s^0 \to \mu^+\,\mu^-)$ is $(3.35 \pm 0.32) \times 10^{-9}$ [28]. The CDF experiment has reported an upper bound on this branching ratio of 4.47×10^{-8} at 90% C.L. [29].

These two decays provide complementary information about the NP operators. The contribution of the SP couplings to $\bar{B} \to X_s \mu^+ \mu^-$ is suppressed by the small coefficient $B_{SP} \sim 10^{-9}$, as compared to $B_{SM} \sim 10^{-6}$. As a result, the constraints on the SP coefficients from this decay are rather weak. On the other hand, the coefficient of the tensor couplings, B_T, is an order of magnitude larger than B_{SP}, while the VA operators interfere with those of the SM ($B_{SM\text{-}VA}$). Therefore, this decay is sensitive mainly to the new VA and T couplings. In contrast, the main contributions to $\bar{B}_s^0 \to \mu^+ \mu^-$ are precisely from the SP operators: there is no contribution from the vector couplings $R_V^{(\prime)}$, the axial-vector contribution proportional to $R_A^{(\prime)}$ is suppressed by m_μ / m_{B_s}, and there is no tensor piece since $\langle 0 | \bar{s} \sigma_{\mu\nu} b | B_s^0(p) \rangle$ vanishes.

The constraints on the new VA couplings coming from $B(\bar{B} \to X_s\,\mu^+\,\mu^-)$ involve the interference terms between the SM and the NP. When R_V and R_A are constrained to be real, the allowed region in the R_V-R_A parameter space therefore looks like an annulus, as shown in the left panel of Fig. 2, as long as no other NP couplings are present. When the couplings R_V' and R_A' are also permitted to be nonzero real numbers, the allowed region takes the form of an elliptical disc, as shown in the right panel of Fig. 2. The $R_{V,A}'$ couplings do not interfere with the SM, so their constraints take the form of an elliptical disc in the R_V'-R_A' plane. If $R_{V,A}$ are not present, the constraints are approximately

$$|R_V'|^2 + |R_A'|^2 \leq 16.8\,, \quad (3.14)$$

while if $R_{V,A}$ are allowed, these constraints are somewhat weakened to

$$|R_V'|^2 + |R_A'|^2 \leq 39.7\,. \quad (3.15)$$

The constraints on the tensor operators also come entirely from $B(\bar{B} \to X_s\,\mu^+\,\mu^-)$ and are rather tight. We find that the allowed values of the new tensor couplings are restricted to

$$|C_T|^2 + 4|C_{TE}|^2 \leq 1.3\,. \quad (3.16)$$

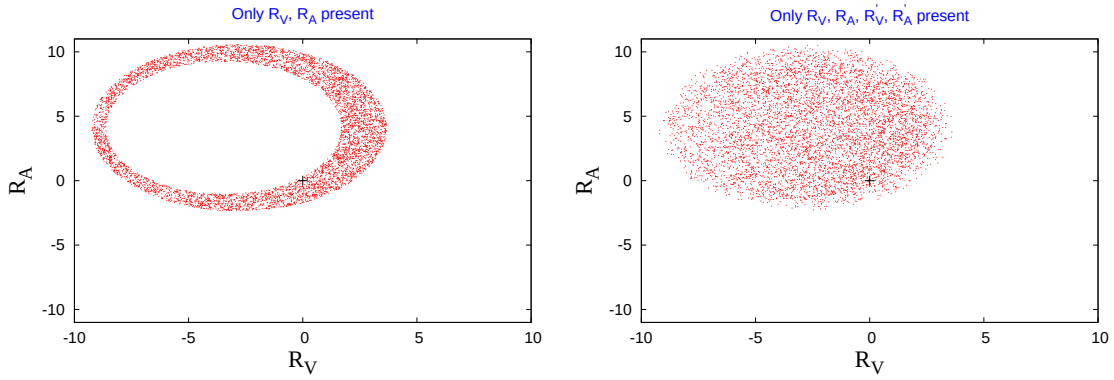

Figure 2: Allowed parameter space in the R_V-R_A plane when $R'_{V,A}$ couplings are absent (left panel) and present (right panel). All the couplings have been taken to be real. The "+" corresponds to the SM.

For the SP operators, the present upper bound on $B(\bar{B}_s^0 \to \mu^+\mu^-)$ gives the limit

$$|R_S - R'_S|^2 + |R_P - R'_P|^2 \leq 0.44 \,, \tag{3.17}$$

where we have used $|V_{ts}| = (0.0407 \pm 0.0010)$ [30] and $f_{B_s} = (0.243 \pm 0.011)$ GeV [31]. If only $R_{S,P}$ or $R'_{S,P}$ are present, this constitutes a severe constraint on the NP couplings. However, if both types of operators are present, these bounds can be evaded due to cancellations between the $R_{S,P}$ and $R'_{S,P}$. In that case, the constraints on these couplings come mainly from $B(\bar{B} \to X_s\,\mu^+\,\mu^-)$, and are rather weak:

$$|R_S|^2 + |R_P|^2 < 45 \,, \quad R'_S = R_S \,, \quad R'_P = R_P \,. \tag{3.18}$$

However, we shall ignore such fine-tuned situations.

3.3 Forward-backward asymmetry and the differential branching ratio

The double differential decay rate $d^2\Gamma/dq^2 d\cos\theta$, calculated by substituting the matrix element from Eq. (3.5) into Eq. (2.6), in turn leads to the calculation of dB/dq^2 and $A_{\rm FB}(q^2)$.

The differential branching ratio is given by

$$\frac{dB}{dq^2} = \frac{G^2\alpha^2}{2^{14}}\frac{1}{\pi^5}|V_{tb}V_{ts}^*|^2 m_B \tau_B \sqrt{\lambda}\,\Theta \,, \tag{3.19}$$

where τ_B is the lifetime of B meson. The quantity Θ has the form

$$\Theta = \frac{1}{3\hat{r}}\Big[X_{SP} + X_{VA} + X_T + X_{SP\text{-}VA} + X_{SP\text{-}T} + X_{VA\text{-}T}\Big] \,, \tag{3.20}$$

where the X terms are classified according to the contributions they contain coming from scalars-pseudoscalars, vectors-axial vector and tensor operators. Their complete

expressions are given in Appendix A. Note that the SM contribution is contained inside the X terms labeled by VA. Therefore whenever the new VA operators are absent, the $X_{VA}, X_{SP\text{-}VA}, X_{VA\text{-}T}$ terms will be referred to as $X_{SM}, X_{SP\text{-}SM}, X_{SM\text{-}T}$, respectively, for clarity.

The forward-backward asymmetry can also be written in the form

$$A_{\rm FB}(q^2) = 2m_B \frac{\sqrt{\lambda}}{\hat{r}\Theta}\Big[Y_{SP} + Y_{VA} + Y_T + Y_{SP\text{-}VA} + Y_{SP\text{-}T} + Y_{VA\text{-}T}\Big] \,, \tag{3.21}$$

with the complete expressions for the Y terms given in Appendix A. As in the case of the X terms, whenever new VA operators are absent, we refer to the $Y_{VA}, Y_{SP\text{-}VA}, Y_{VA\text{-}T}$ terms as $Y_{SM}, Y_{SP\text{-}SM}, Y_{SM\text{-}T}$, respectively.

Most of the qualitative features of the NP impact on the above quantities can be easily understood if we use simplified expressions that neglect terms proportional to the small quantities $\hat{m}_l$ and $\hat{r}$ at appropriate places. (Note that this may not be valid for extremely low values of q^2.) With this approximation, the terms in dB/dq^2 simplify to

$$\begin{aligned}
X_{SP} &\approx 3(|B_1|^2 + |B_2|^2) m_B^2 z\lambda \,, \\
X_{VA} &\approx 2(|C|^2 + |G|^2) m_B^2 \lambda^2 + 2(|B|^2 + |F|^2)(12\hat{r}z + \lambda) \\
&\qquad - 4{\rm Re}(FG^* + BC^*) m_B^2 (1-z)\lambda \,, \\
X_T &\approx |C_T|^2 (\text{Quadratic terms in } B_3, B_4, T_1) \\
&\qquad + |C_{TE}|^2 (\text{Quadratic terms in } B_3, B_4, T_1) \,.
\end{aligned} \tag{3.22}$$

The three interference terms, $X_{SP\text{-}VA}, X_{SP\text{-}T}$ and $X_{VA\text{-}T}$ vanish in this approximation, indicating that dB/dq^2 can be thought of as the simple addition of the SP, VA, and T contributions.

With the same approximations, the only surviving Y terms in $A_{\rm FB}(q^2)$ are

$$\begin{aligned}
Y_{VA} &\approx -4m_B \hat{r} z {\rm Re}\Big(A^* F + B^* F_1\Big) \\
Y_{SP\text{-}T} &\approx m_B z {\rm Re}\Big(2B_1^* C_{TE} + B_2^* C_T\Big) \times \\
&\qquad \Big((2B_3 - 4T_1)(z-1) + B_4 m_B^2 \lambda\Big) \,.
\end{aligned} \tag{3.23}$$

The chiral structure of the operators ensures that all the other terms are suppressed by $\hat{m}_l = m_l/m_B \approx 0.02$.

The approximate expressions in Eqs. (3.22) and (3.23) imply that

- New interactions of the type only SP or only T only always increase Θ, and hence dB/dq^2, but do not contribute to Y. As a result, $A_{\rm FB}(q^2)$ always decreases in magnitude with such new physics.

- New VA interactions, or an SP-T combination, is required in order to enhance $A_{\rm FB}(q^2)$ significantly, or to change its sign.

Note that the SP-T contribution was already considered in Ref. [32] in the context of the inclusive decay $\bar{B} \to X_s l^+ l^-$. However, it was concluded that its effect was basically to increase the branching ratio while leaving unchanged the integrated $A_{\rm FB}$. For this reason, this contribution was disregarded in subsequent papers such as Ref. [33]. However, as we shall show here, this type of NP can in fact shift the differential asymmetry $A_{\rm FB}(q^2)$ towards the Belle data.

In order to determine the numerical values of dB/dq^2 and $A_{\rm FB}(q^2)$, we need to calculate the form factors. The theoretical predictions for $A_{\rm FB}(q^2)$ are rather uncertain in the intermediate region (7 GeV$^2 \le q^2 \le$ 12 GeV^2) due to nearby charmed resonances. The predictions are relatively more robust for lower and higher q^2. We therefore concentrate on calculating $A_{\rm FB}(q^2)$ in the low-q^2 (1 GeV$^2 \le q^2 \le$ 6 GeV^2) and the high-q^2 ($q^2 \ge 14.4$ GeV^2) regions.

3.3.1 Form factors in the low-q^2 region

When the initial hadron contains the heavy b quark, and the final meson has a large energy, the hadronic form factors can be expanded in the small ratios $\Lambda_{\rm QCD}/m_b$ and $\Lambda_{\rm QCD}/E$, where $\Lambda_{\rm QCD}$ is the strong interaction scale and E is the energy of the light meson. Neglecting corrections of $O(\alpha_s)$, the 7 a-priori independent $B \to K^*$ form factors [see Eqs. (A.1)–(A.5)] can be expressed in terms of two universal form factors $\xi_\perp(q^2)$ and $\xi_\parallel(q^2)$ [34, 35, 36, 37]:

$$\begin{aligned}
A_1(q^2) &= \frac{2E_{K^*}}{m_B + m_{K^*}}\,\xi_\perp(q^2)\,, \\
A_2(q^2) &= \frac{m_B}{m_B - m_{K^*}}\left[\xi_\perp(q^2) - \xi_\parallel(q^2)\right], \\
A_0(q^2) &= \frac{E_{K^*}}{m_{K^*}}\,\xi_\parallel(q^2)\,, \\
V(q^2) &= \frac{m_B + m_{K^*}}{m_B}\,\xi_\perp(q^2)\,, \\
T_1(q^2) &= \xi_\perp(q^2)\,, \\
T_2(q^2) &= \frac{2E_{K^*}}{m_B}\,\xi_\perp(q^2)\,, \\
T_3(q^2) &= \xi_\perp(q^2) - \xi_\parallel(q^2)\,.
\end{aligned} \tag{3.24}$$

Here, E_{K^*} is the energy of the K^* in the B rest frame:

$$E_{K^*} \simeq \frac{m_B}{2}\left(1 - \frac{q^2}{m_B^2}\right). \tag{3.25}$$

The q^2-dependence of the form factors is assumed to be [9]

$$\xi_\parallel(q^2) = \xi_\parallel(0)\left[\frac{1}{1 - q^2/m_B^2}\right]^2 \quad , \quad \xi_\perp(q^2) = \xi_\perp(0)\left[\frac{1}{1 - q^2/m_B^2}\right]^3 , \tag{3.26}$$

	$f(0)$	c_1	c_2
A_1	0.337	0.602	0.258
A_2	0.282	1.172	0.567
A_0	0.471	1.505	0.710
V	0.457	1.482	1.015
T_1	0.379	1.519	1.030
T_2	0.379	0.517	0.426
T_3	0.260	1.129	1.128

Table 1: Central values of the parameters of the form factors for the $B \to K^*$ transition [see Eq. (3.28)] [22]

as predicted by power counting in the heavy-quark limit. In our analysis, we take [9]

$$\xi_\parallel(0) = 0.16 \pm 0.03 \quad , \quad \xi_\perp(0) = 0.26 \pm 0.02 \; . \tag{3.27}$$

The previous relations get corrections of $O(\alpha_s)$ [9] and possible Λ/m_b contributions. However, for our analysis it is sufficient to stay at LO to determine which new couplings can induce a clear change of behavior of $A_{\rm FB}(q^2)$.

3.3.2 Form factors in the high-q^2 region

In order to estimate $A_{FB}(q^2)$ in the high-q^2 region, we take the form factors calculated in the QCD sum rule approach [22]. The z ($\equiv q^2/m_B^2$) dependence of the 7 form factors is given by

$$f(z) = f(0)\, \exp(c_1 z + c_2 z^2) \; . \tag{3.28}$$

The central values of the parameters $f(0)$, c_1 and c_2 for each form factor are given in Table 1. In order to take into account form factor uncertainties, we have used the maximum and minimum allowed values of the parameters $f(0)$, c_1 and c_2 as given in [22].

4. $A_{\rm FB}(q^2)$ and dB/dq^2 in the Presence of NP

In this section, we examine the predictions for $A_{\rm FB}(q^2)$ and dB/dq^2 in the presence of NP operators. We consider different Lorentz structures of NP, as well as their combinations, and examine the implications using the constraints on the new couplings obtained in Sec. 3.2. In all figures, we show $A_{\rm FB}(q^2)$ and dB/dq^2 for representative values of the NP couplings. The representative values have been chosen such that the maximum and minimum allowed values of $A_{\rm FB}(q^2)$ and dB/dq^2, as well as cases with interesting variations of $A_{\rm FB}(q^2)$, are displayed. The same color (type) of line

in all four panels of a figure corresponds to the same values of NP parameters. In addition, for comparison, we also show the experimental data. For this numerical analysis, we have taken the NP couplings to be real.

4.1 VA new-physics operators

From the discussion following Eq. (3.23), it is expected that NP in the form of vector-axial vector operators may be able to enhance $A_{\rm FB}(q^2)$ or change its sign. However, depending on whether the NP couplings are $R_{V,A}$ or $R'_{V,A}$, the effect on $A_{\rm FB}(q^2)$ will have different features. In this section, we shall sequentially consider the scenarios in which (i) only $R_{V,A}$ couplings are present, (ii) only $R'_{V,A}$ couplings are present, and (iii) both types of couplings are allowed.

4.1.1 Only R_V, R_A couplings present

Fig. 3 shows the results when the only NP couplings present are R_V and R_A. The following remarks are in order:

- For certain values of R_V and R_A, $A_{\rm FB}(q^2)$ can be either always positive (a possible solution for the Belle observation) or always negative. That is, for these cases there is no zero crossing point. This is easily explained because, in the presence of R_V and R_A, Eq. (2.8) becomes at LO

$$\mathrm{Re}(C_9^{\rm eff}(q_0^2)) + R_V = -\frac{2m_B m_b}{q_0^2} C_7^{\rm eff} \ . \tag{4.1}$$

  Then R_V can unbalance the contribution from $C_9^{\rm eff}$, so that there is no solution, and consequently no zero. The effect of R_A is simply to rescale $A_{\rm FB}$.

- In general the zero crossing can be anywhere in the whole q^2 range. The crossing can be negetive to positive (positive crossing) or positive to negative(negative crossing).

- It is possible to have a large $A_{\rm FB}(q^2)$ while being consistent with the SM prediction of the differential branching ratio dB/dq^2. This is explained by the different type of contributions entering the X and Y terms in Eqs. (3.22) and (3.23).

- The differential branching ratio dB/dq^2 can be increased in the low-q^2 region by up to 50%. However, in such cases, $A_{\rm FB}(q^2)$ becomes highly negative at high q^2, inconsistent with the current data. This suggests that, in general, dB/dq^2 will not be affected in this scenario.

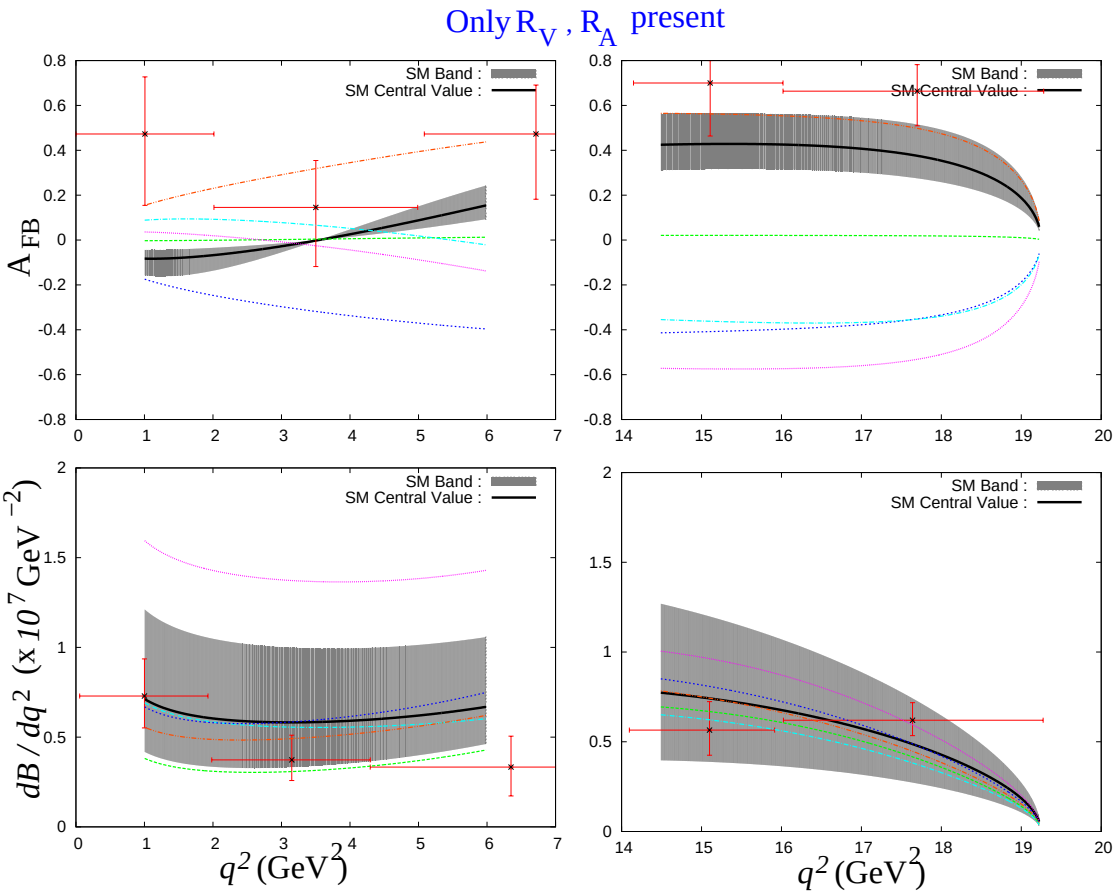

Figure 3: The left (right) panels of the figure show $A_{\rm FB}(q^2)$ and dB/dq^2 in the low-q^2 (high-q^2) region, in the scenario where only R_V and R_A couplings are present. The different (colored) curves correspond to different choices of the R_V and R_A couplings inside their allowed region. For comparison, the experimental data are also displayed.

4.1.2 Only R'_V, R'_A couplings present

Fig. 4 shows the results when the only NP couplings present are R'_V and R'_A. From the figure, we make the following observations:

- For certain values of R'_V and R'_A, the position of the zero crossing is shifted significantly, but it is always a positive crossing, since $A_{\rm FB}(q^2)$ is highly negative in the low-q^2 region. This behavior can be understood from Eq. (2.8), which in the presence of R'_V and R'_A becomes at LO

$$Re(C_9^{\rm eff}(q_0^2)) - \frac{R'_V R'_A}{C_{10}} = -\frac{2m_B m_b}{q_0^2} C_7^{\rm eff} \ . \tag{4.2}$$

  In order to counteract the contribution from $C_9^{\rm eff}$, we must have $|R'_V R'_A/C_{10}| >$ Re$(C_9^{\rm eff})$. However, this is not allowed by the present measurement of the

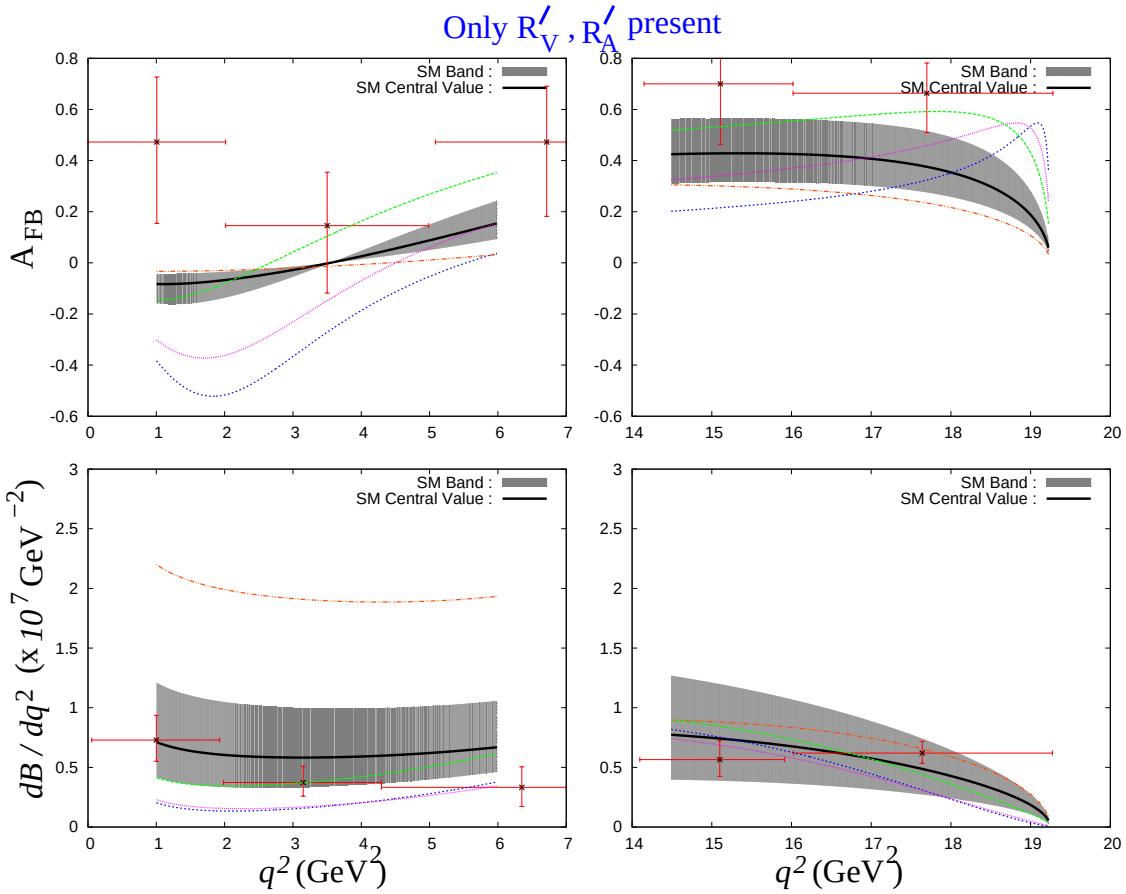

Figure 4: The left (right) panels of the figure show $A_{\rm FB}(q^2)$ and dB/dq^2 in the low-q^2 (high-q^2) region, in the scenario where only R'_V and R'_A terms are present.

branching ratio of $\bar{B} \to X_s\mu^+\mu^-$. Hence, the zero crossing is always SM-like, i.e. always positive, which is not favored by the Belle data.

- It is possible to have dB/dq^2 consistent with the SM, simultaneously with a larger $A_{\rm FB}(q^2)$ than the SM (up to 0.6), but only near the high-q^2 end.

- dB/dq^2 at low q^2 can be enhanced by up to a factor of 2, but then $A_{\rm FB}(q^2)$ would become very small. On the other hand, dB/dq^2 at low q^2 can decrease by up to 50%, but this would result in a large negative value of $A_{\rm FB}(q^2)$ in this region.

4.1.3 All VA couplings present

Fig. 5 shows $A_{\rm FB}(q^2)$ and dB/dq^2 when all the VA NP couplings, R_V, R_A, R'_V, R'_A are present. The following different results are obtained depending on the choice of the couplings:

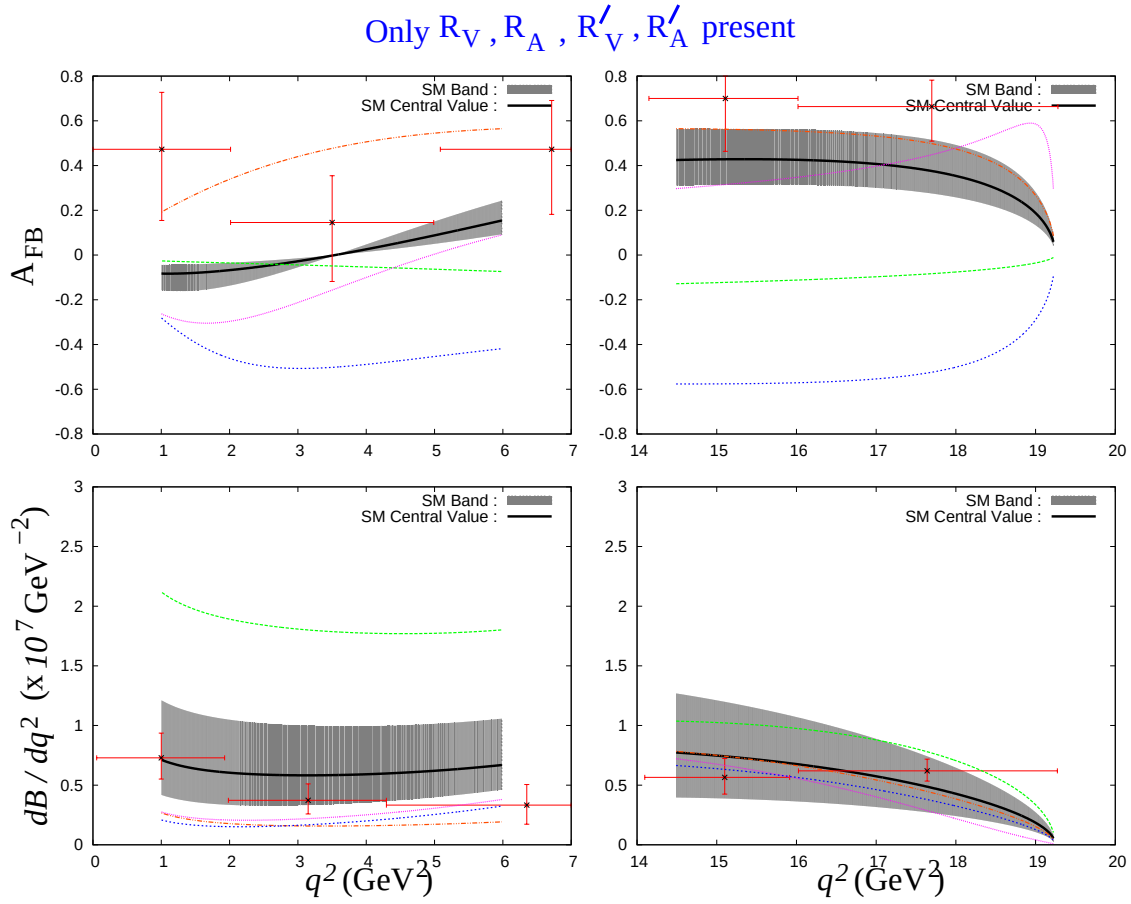

Figure 5: The left (right) panels of the figure show $A_{\rm FB}(q^2)$ and dB/dq^2 in the low-q^2 (high-q^2) region, in the scenario where both $R_{V,A}$ and $R'_{V,A}$ terms are present.

- For certain values of the couplings, $A_{\rm FB}(q^2)$ can be either always positive or always negative. That is, there is no zero crossing point.
- The zero crossing can be anywhere in the whole q^2 range. It can be either positive or negative.
- Particularly interesting is the case of the top curve in $A_{\rm FB}(q^2)$ of Fig. 5. Here we see that it is possible to have large $A_{\rm FB}(q^2)$ at low q^2, along with the suppression of dB/dq^2 in this region, as indicated by the Belle data.
- It is possible to have dB/dq^2 consistent with the SM, simultaneously with a larger $A_{\rm FB}(q^2)$ than the SM (up to 0.6) in the whole q^2 region.

The key point here is that, in order to reproduce the current experimental data, one needs *both* $R_{V,A}$ and $R'_{V,A}$ couplings. They change $A_{\rm FB}(q^2)$ appropriately in the low- and high-q^2 regions, respectively. At present, the errors on the measurements are

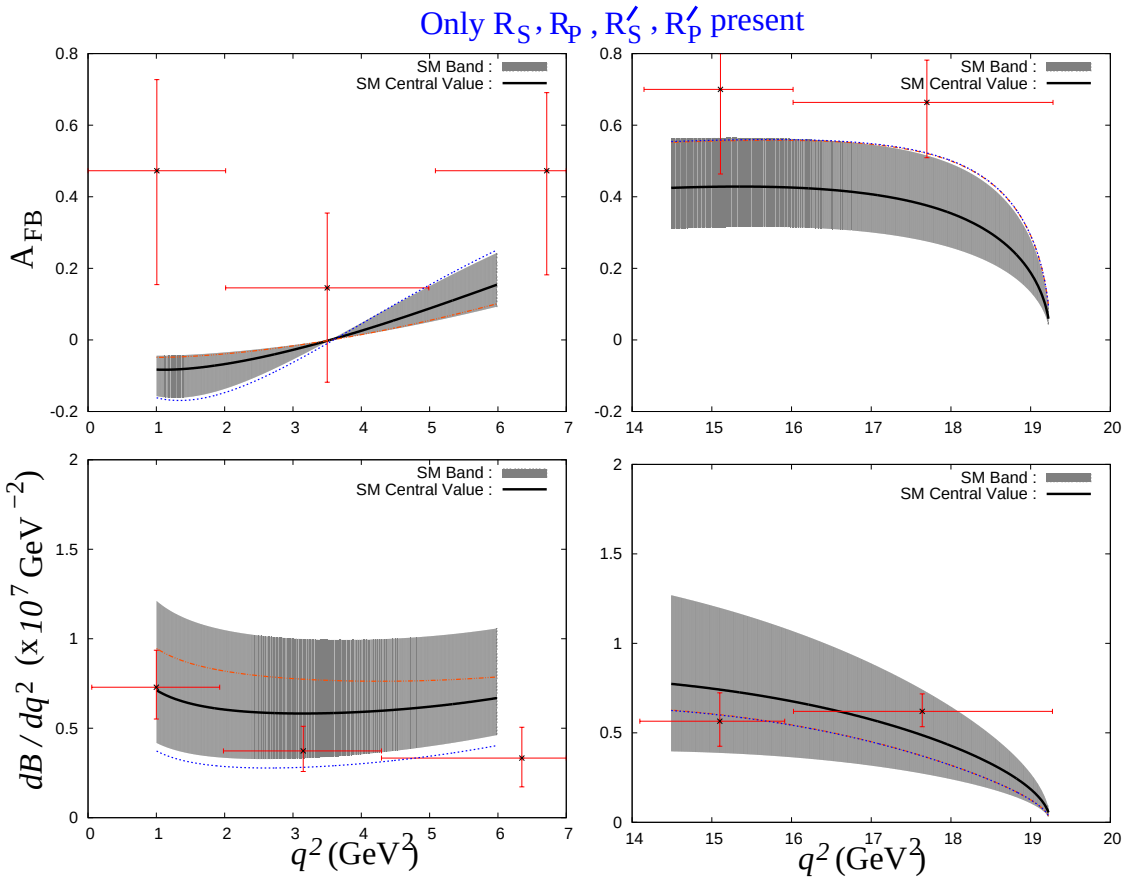

Figure 6: The left (right) panels of the figure show $A_{\rm FB}(q^2)$ and dB/dq^2 in the low-q^2 (high-q^2) region, in the scenario where both $R_{S,P}$ and $R'_{S,P}$ terms are present.

quite large. However, if future experiments reproduce the current central values with greater precision, this will put important constraints on any NP model proposed to explain the data.

One NP model which contains VA operators (both $R_{V,A}$ and $R'_{V,A}$) involves Z'-mediated FCNCs. A recent analysis [38] specifically notes that the measurement of $A_{\rm FB}(q^2)$ can be explained within this model. From the above analysis, we see that this is one case of a more general result.

4.2 Only SP new-physics operators

From the discussion following Eq. (3.23), NP involving only SP operators is expected to decrease $A_{\rm FB}(q^2)$. Fig. 6 shows the results when all the SP NP couplings, R_S, R_P, R'_S, R'_P are present. There we see that:

- The SP operators have unobservably small effects on $A_{\rm FB}(q^2)$ and dB/dq^2.
- There is always a SM-like zero crossing.

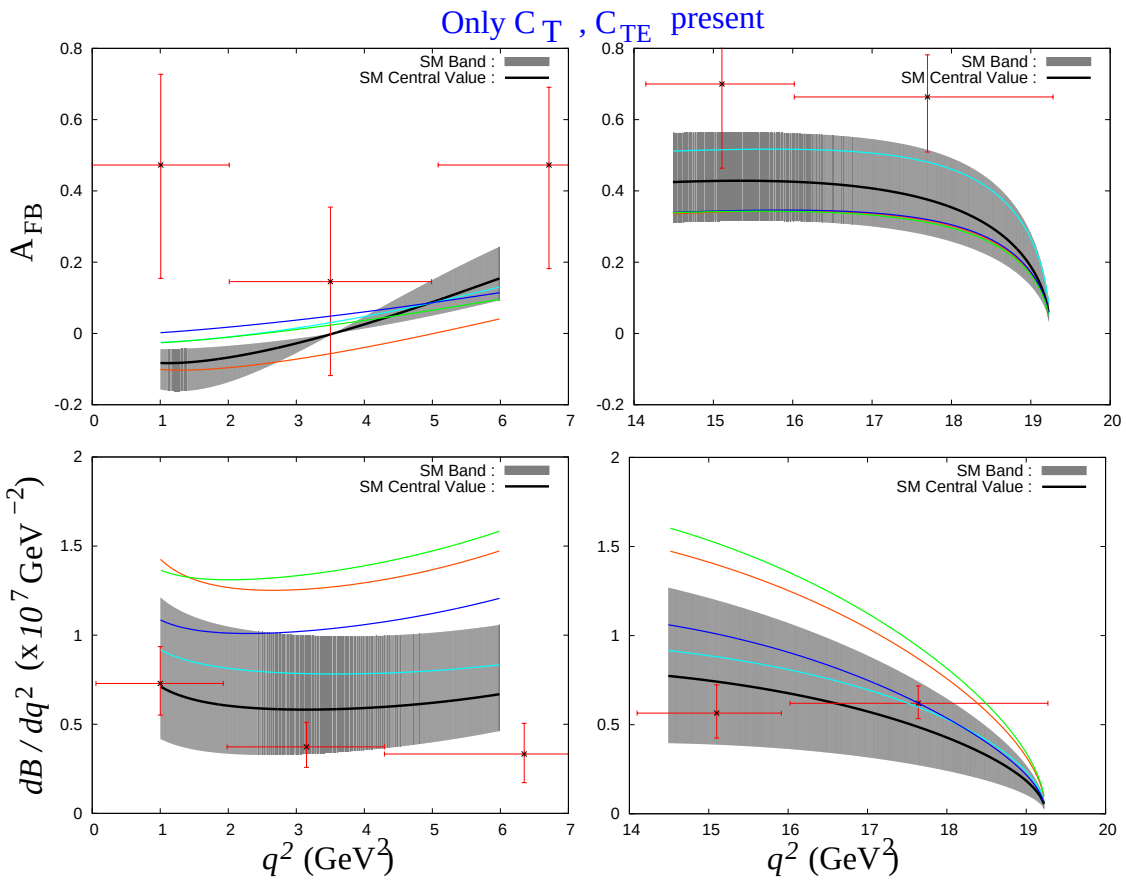

Figure 7: The left (right) panels of the figure show $A_{\rm FB}(q^2)$ and dB/dq^2 in the low-q^2 (high-q^2) region, when NP is present only in the form of tensor operators.

Contribution to $A_{\rm FB}(q^2)$ in this scenario can in principle come from the terms Y_{SP} and Y_{SP-SM} in Eq. (3.21). However as as can be seen from Eq. (A.14), Y_{SP} vanishes identically while Y_{SP-SM} is $\hat{m}_l$-suppressed. In addition, the couplings $R_{S,P}$ and $R'_{S,P}$ are strongly constrained from the upper bound on $B(\bar{B}_s \to \mu^+\mu^-)$. For both of these reasons, these operators have a negligible effect on $A_{\rm FB}(q^2)$ and dB/dq^2.

4.3 Only T new-physics operators

For the case where only tensor NP operators are added, $A_{\rm FB}(q^2)$ is expected to be suppressed, as the discussion following Eq. (3.23) suggests. Fig. 7 shows the results in this scenario. The following remarks are in order:

- $A_{\rm FB}(q^2)$ is in general suppressed in both the low- and high-q^2 regions, as expected.

- The zero crossing can be anywhere in the entire q^2 range, or it may disappear altogether. Whenever it is present, it is always a positive crossing like the

SM. This shift of zero crossing shows that the $\hat{m}_l$-suppressed $Y_{SM\text{-}T}$ term in Eq. (A.14) is important. In the absence of this term, the zero crossing point would have remained the same as the SM.

- dB/dq^2 is enhanced. The enhancement can be significant, up to a factor of 2.

Contributions to $A_{\rm FB}(q^2)$ in this scenario are expected from the terms Y_T and $Y_{SM\text{-}T}$ in Eq. (3.21). However, as can be seen from Eq. (A.14), Y_T vanishes identically, while $Y_{SM\text{-}T}$ is $\hat{m}_l$-suppressed. On the other hand, the term X_T has no such suppression, and it contributes to Θ, resulting in an enhancement of dB/dq^2. The increased value of Θ also leads to the suppression of $A_{\rm FB}(q^2)$ in Eq. (3.21). In some regions of parameter space, though, the contribution of the many terms in $Y_{SM\text{-}T}$ is no longer negligible. In such cases, the zero crossing shifts and $A_{\rm FB}(q^2)$ at low q^2 can become positive.

4.4 Simultaneous SP and T new-physics operators

The discussion following Eq. (3.23) suggests that if both SP and T NP couplings are present simultaneously, there is the possibility that $A_{\rm FB}(q^2)$ is enhanced or changes sign. In this section, we quantitatively check if such an enhancement can take the $A_{\rm FB}(q^2)$ predictions closer to the current Belle measurements. We take the couplings $R_S, R_P, R'_S, R'_P, C_T, C_{TE}$ to be nonvanishing, and show the results in Fig. 8. From the figure, we see the following:

- There is some parameter space of couplings where $A_{\rm FB}(q^2)$ is positive everywhere, i.e. there is no zero crossing.
- The absolute value of $A_{\rm FB}(q^2)$ cannot be enhanced above the SM, except at very low q^2. Even here, the enhancement is very small.
- dB/dq^2 is enhanced. The enhancement can be significant, up to a factor of 2.

Since the contribution to $A_{\rm FB}(q^2)$ here comes from two terms, the $\hat{m}_l$-suppressed (but not negligible) $Y_{SM\text{-}T}$ and the not-$\hat{m}_l$-suppressed $Y_{SP\text{-}T}$ [see Eq. (A.14)], $A_{\rm FB}(q^2)$ is now expected to be larger than in the scenario with only T operators. Though this trend is observed in general, the severe restrictions on the SP couplings do not allow $A_{\rm FB}(q^2)$ to become significantly more than the SM in magnitude. Still, $A_{\rm FB}(q^2)$ can be influenced enough to cause a vanishing of zero crossing and positive $A_{\rm FB}(q^2)$ at low q^2.

Certain NP models can contribute to the SP-T mechanism, though there are caveats. In the MSSM, tensor operators in $b \to s\,\mu^+\,\mu^-$ are induced from photino and zino box diagrams. However, their couplings are subleading in $\tan\beta$ with respect to the Higgs penguins [39]. Tensor operators can also be induced in leptoquark models by tree-level scalar leptoquark exchange (and a Fierz transformation). However, the

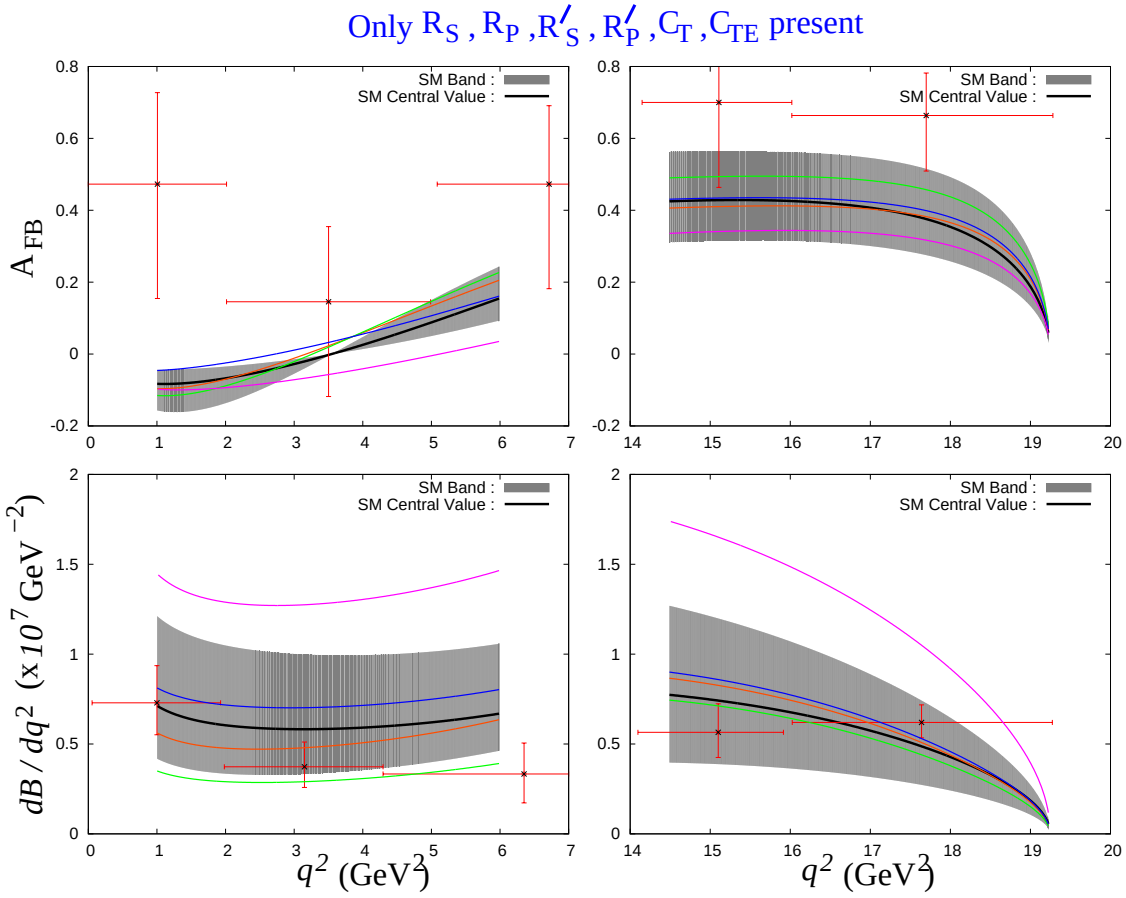

Figure 8: The left (right) panels of the figure show $A_{\rm FB}(q^2)$ and dB/dq^2 in the low-q^2 (high-q^2) region, when NP present is in the form of SP and T operators.

tensor couplings are suppressed by the ratio of the Higgs vacuum expectation value and the scalar leptoquark mass [40].

4.5 Other combinations of VA, SP, and T operators

The pattern of the effect of NP Lorentz structures on $A_{\rm FB}(q^2)$ and dB/dq^2 is now clear, so that the results from the remaining combinations of operators can be discerned straightforwardly. The addition of VA operators allows for an enhanced $A_{\rm FB}(q^2)$ and a moderate enhancement of dB/dq^2. The addition of SP operators does not affect the results much due to the severe restrictions on the SP couplings. The addition of T operators tends to enhance dB/dq^2 strongly and decrease $A_{\rm FB}(q^2)$ at the same time. In addition, we have found that specific combinations of operators, such as SP-T, collaborate, with the results approaching the experimental data.

4.6 Other new-physics sources that may affect $A_{\rm FB}(q^2)$

In addition to the two NP mechanisms which have been found to significantly affect

$A_{\rm FB}(q^2)$ (new VA operators, or an SP-T operator combination), there are two additional mechanisms that can in principle lead to the same effect. We comment on them here.

In the first mechanism, NP is assumed to affect the ordinary dipole operator $O_7 = \bar{s}\sigma^{\alpha\beta}P_R b\, F_{\alpha\beta}$. In this case, the Wilson coefficient $C_7^{\rm eff}$ will be modified. This will result in the shifting of the position of zero crossing, as can be seen from Eq. (2.8). Now, there has been no hint of NP in the radiative decays $\bar{B} \to X_s\gamma, \bar{K}^{(*)}\gamma$, imposing strong constraints on $|C_7^{\rm eff}|$. Still, if the effect of the NP is to simply reverse the sign of $C_7^{\rm eff}$, then Eq. (2.8) would not be fulfilled, and a positive $A_{\rm FB}(q^2)$ would be produced for low q^2. However, this solution can be ruled out at 3σ from the decay rate of $\bar{B} \to X_s\ell^+\ell^-$ [41]. This constraint can be evaded if the couplings R_V and R_A are also taken to be nonzero. Thus, if there is NP in O_7 whose sole effect is to reverse the sign of $C_7^{\rm eff}$, *and* the NP couplings R_V and R_A are present, it is possible to reproduce the $A_{\rm FB}(q^2)$ data. In other words, a great many things have to happen perfectly for this mechanism to work. We consider this very unlikely, and so consider this mechanism less plausible.

Another NP possibility, independent of those included in Eq. (3.1), is the addition of the chirally-flipped operator $O_7' = \bar{s}\sigma^{\alpha\beta}P_L b\, F_{\alpha\beta}$. The impact of this on $A_{\rm FB}(q^2)$, together with other observables, was studied in Ref. [17]. There it was found that $A_{\rm FB}(q^2)$ does not significantly deviate from the SM prediction if only this operator is introduced. We therefore exclude the possibility of NP giving rise to O_7'.

5. Discussion and Summary

Motivated by the recent Belle measurement of the forward-backward asymmetry $A_{\rm FB}(q^2)$ in $\bar{B} \to \bar{K}^*\mu^+\mu^-$, indicating a discrepancy with the SM, we calculate this quantity in the presence of new physics (NP) in the low- and high-q^2 regions. We perform a systematic model-independent analysis, allowing for new vector-axial vector (VA), scalar-pseudoscalar (SP) and tensor (T) couplings. Using the constraints on the new couplings from other related decays, we determine how the NP affects $A_{\rm FB}(q^2)$ and the differential branching fraction dB/dq^2. This allows us to compare the effects of different NP Lorentz structures.

The present Belle data [10] hint at a positive $A_{\rm FB}(q^2)$ in the whole q^2 region, i.e. no zero crossing as predicted by the SM. Though we look for NP sources that can give rise to this feature, our analysis is more general. Indeed, the discrepancy with the SM prediction is only at the 2σ level, and this could change with more precise measurements in the future. We therefore focus on identifying unique features of all the sources of NP, and the patterns of their effects on $A_{\rm FB}(q^2)$ and dB/dq^2. We observe that the effects on these two quantities are correlated, which could enable the discrimination between different NP sources with future data.

We show, through analytical approximations and numerical calculations, that two kinds of NP scenarios can give rise to a positive $A_{\rm FB}(q^2)$ in the whole q^2 range:

- NP VA operators can enhance $A_{\rm FB}(q^2)$ in the whole q^2 region and keep its value positive. Both $R_{V,A}$ and $R'_{V,A}$ couplings are necessary. The terms involving $R_{V,A}$ can make $A_{\rm FB}(q^2)$ positive at low q^2, while the terms involving $R'_{V,A}$ can increase $A_{\rm FB}(q^2)$ above its SM value in the high-q^2 region. It is therefore possible to very closely reproduce the Belle data. However, in general this can also lead to a significant suppression of dB/dq^2. This is because the VA operators can interfere with the SM operators without $\hat{m}_l$ suppression, and a destructive interference in dB/dq^2 would tend to enhance $A_{\rm FB}(q^2)$. Still, $A_{\rm FB}(q^2)$ values close to the Belle data and dB/dq^2 consistent with the SM predictions are also possible in this scenario.

- The T operators can influence $A_{\rm FB}(q^2)$ in the low-q^2 region sufficiently to change its sign and make it positive. They still cannot enhance the magnitude of the asymmetry significantly, since the interference of these operators with the SM is $\hat{m}_l$-suppressed. Moreover, the addition of these operators can only enhance dB/dq^2. The simultaneous presence of SP operators allows interference terms between SP and T operators that are not $\hat{m}_l$-suppressed, and tends to take $A_{\rm FB}(q^2)$ closer to the Belle data. However this improvement is marginal, since the SP couplings are highly constrained from the upper bound on $B(\bar{B}_s \to \mu^+\mu^-)$.

If the Belle anomaly remains in future measurements, the NP source has to be one of the above two (or the less plausible mechanism involving a conspiracy between O_7, R_V and R_A operators to flip the sign of O_7). We will be able to distinguish between them through the following observations:

- $A_{\rm FB}(q^2)$ at high q^2: the scenarios with only T operators or an SP-T combination cannot give rise to an enhanced $A_{\rm FB}(q^2)$ at high q^2. Such a situation necessarily requires VA operators, in particular involving the couplings $R'_{V,A}$.

- Correlation with dB/dq^2: the T-only or SP-T scenarios cannot in general suppress dB/dq^2 much below its SM value, while the VA scenario will be able to do this.

- Correlation with $A_{\rm FB}(q^2)$ in $\bar{B} \to \bar{K}\mu^+\mu^-$: within the SM, $A_{\rm FB}(q^2)$ in $\bar{B} \to \bar{K}\mu^+\mu^-$ is consistent with zero since the hadronic matrix element for the $B \to K$ transition does not get any contribution from axial-vector current. For the same reason, new VA operators cannot contribute to $A_{\rm FB}(q^2)$ in $\bar{B} \to \bar{K}\mu^+\mu^-$. Hence, the only possible contribution to the asymmetry can be from SP or T operators. In Ref. [20], it was shown that, if the NP is only in the form of SP

or T operators, then the additional contribution to $A_{\rm FB}(q^2)$ is proportional to the lepton mass and hence is highly suppressed. However, if both SP and T operators are present simultaneously, then $A_{\rm FB}(q^2)$ in $\bar{B} \to \bar{K}\mu^+\mu^-$ can be as large as 15%. Thus, if the SP-T scenario is responsible for $A_{\rm FB}(q^2)$ in $\bar{B} \to \bar{K}^*\mu^+\mu^-$, we will also see a large $A_{\rm FB}(q^2)$ in $\bar{B} \to \bar{K}\mu^+\mu^-$. This measurement may also help distinguishing between the T-only and SP-T scenarios.

Even if the Belle anomaly does not persist, or shows some other features, our analysis enables us to recognize patterns of the effects of VA, SP and T operators on $A_{\rm FB}(q^2)$ and dB/dq^2:

- New VA operators can interfere with the SM operators without $\hat{m}_l$ suppression, and hence are the only ones that can reduce dB/dq^2 substantially below the SM prediction. They can also interfere among themselves and with the SM operators to give rise to a large magnitude for $A_{\rm FB}(q^2)$, with either sign. They can influence the zero crossing point q_0 by changing the SM relation between $C_9^{\rm eff}$ and $C_7^{\rm eff}$ that determines its value at LO.

- SP operators always tend to enhance dB/dq^2, since their interference terms with the SM or VA operators are $\hat{m}_l$-suppressed. The contribution of only SP operators to $A_{\rm FB}(q^2)$ is also $\hat{m}_l$-suppressed. Moreover, the magnitudes of the SP couplings are severely constrained from the upper bound on $B(\bar{B}_s \to \mu^+\mu^-)$. Therefore, the addition of only SP operators does not significantly affect either dB/dq^2 or $A_{\rm FB}(q^2)$.

- T operators also always tend to enhance dB/dq^2, owing to the $\hat{m}_l$ suppression of their interference with the SM operators. The enhancement can be rather strong – up to a factor of 2 – since the constraints on the couplings are relatively weak. If the NP is only in the form of T operators, then the contribution to $A_{\rm FB}(q^2)$ is also $\hat{m}_l$-suppressed, though the presence of many such terms mean that the total contribution is not insignificant. The net effect is that the scenario with only T operators tends to show a large dB/dq^2 enhancement and $A_{\rm FB}(q^2)$ suppression.

- The simultaneous presence of SP and T operators gives rise to a qualitatively new feature. Though the dB/dq^2 can be enhanced, one also gets an interference term between the SP and T operators that is not $\hat{m}_l$-suppressed. As a result, a substantial effect on $A_{\rm FB}(q^2)$ is possible, though a large effect is not possible due to the restriction on the SP couplings.

Acknowledgments: We thank Marco Musy, F. Mescia and Mitesh Patel for useful discussions. This work was financially supported by NSERC of Canada (AKA, MN, AS, DL). JM acknowledges financial support from the Research Projects CICYT-FEDER-FPA2008-01430, SGR2005-00916, PORT2008.

A. Analytical Calculation of $A_{\rm FB}(q^2)$ and dB/dq^2

The decay amplitude for $\bar{B} \to \bar{K}^* \mu^+ \mu^-$ [Eq. (3.5)] is written in terms of matrix elements of the quark operators. These are [12]

$$\begin{aligned}\langle \bar{K}^*(p_{K^*},\epsilon)|\bar{s}\gamma_\mu(1\pm\gamma_5)b|\bar{B}(p_B)\rangle &= \mp\, i q_\mu \frac{2m_{K^*}}{q^2}\,\epsilon^*\cdot q\left[A_3(q^2)-A_0(q^2)\right] \\ &\pm\, i\epsilon^*_\mu(m_B+m_{K^*})A_1(q^2) \mp\; i(p_B+p_{K^*})_\mu\,\epsilon^*\cdot q\,\frac{A_2(q^2)}{(m_B+m_{K^*})} \\ &-\,\epsilon_{\mu\nu\lambda\sigma}\epsilon^{*\nu}p^\lambda_{K^*}q^\sigma\frac{2V(q^2)}{(m_B+m_{K^*})}\;, \end{aligned} \tag{A.1}$$

where

$$A_3(q^2) \;=\; \frac{m_B+m_{K^*}}{2m_{K^*}}A_1(q^2) - \frac{m_B-m_{K^*}}{2m_{K^*}}A_2(q^2)\;, \tag{A.2}$$

$$\begin{aligned}\langle \bar{K}^*(p_{K^*},\epsilon)|\bar{s}\sigma_{\mu\nu}b|\bar{B}(p_B)\rangle &= i\epsilon_{\mu\nu\lambda\sigma}\Bigg\{-T_1(q^2)\epsilon^{*\lambda}(p_B+p_{K^*})^\sigma \\ &+\frac{(m_B^2-m_{K^*}^2)}{q^2}\Big(T_1(q^2)-T_2(q^2)\Big)\epsilon^{*\lambda}q^\sigma \\ &-\frac{2}{q^2}\Big(T_1(q^2)-T_2(q^2)-\frac{q^2}{(m_B^2-m_{K^*}^2)}\,T_3(q^2)\Big)\epsilon^*\cdot q\,p^\lambda_{K^*}q^\sigma\Bigg\}\;, \end{aligned} \tag{A.3}$$

$$\begin{aligned}\langle \bar{K}^*(p_{K^*},\epsilon)|\bar{s}i\sigma_{\mu\nu}q^\nu(1\pm\gamma_5)b|\bar{B}(p_B)\rangle &= 2\epsilon_{\mu\nu\lambda\sigma}\epsilon^{*\nu}p^\lambda_{K^*}q^\sigma\;T_1(q^2) \\ &\pm\, i\Big\{\epsilon_{*\mu}(m_B^2-m_{K^*}^2)-(p_B+p_{K^*})_\mu\,\epsilon^*\cdot q\Big\}\,T_2(q^2) \\ &\pm\, i\,\epsilon^*\cdot q\left\{q_\mu-\frac{(p_B+p_{K^*})_\mu q^2}{(m_B^2-m_{K^*}^2)}\right\}T_3(q^2)\;, \end{aligned} \tag{A.4}$$

$$\langle \bar{K}^*(p_{K^*},\epsilon)|\bar{s}(1\pm\gamma_5)b|\bar{B}(p_B)\rangle \;=\; \mp\, 2i\frac{m_{K^*}}{m_b}\,\epsilon^*\cdot q\,A_0(q^2)\;. \tag{A.5}$$

Here we have neglected the strange-quark mass. The matrix elements are functions of 7 unknown form factors: $A_{0,1,2}(q^2)$, $V(q^2)$, $T_{1,2,3}(q^2)$.

Using the above matrix elements, the decay amplitude for $\bar{B} \to \bar{K}^* \mu^+ \mu^-$ can be

written as

$$
\begin{aligned}
\mathcal{M} &= \frac{\alpha G_F}{4\sqrt{2}\pi} V_{ts}^* V_{tb} \Bigg[(\bar{u}(p_-)\gamma^\mu v(p_+)) \times \\
&\left\{ -2A\epsilon_{\mu\nu\lambda\sigma}\epsilon^{*\nu} p_{K^*}^\lambda q^\sigma - iB\epsilon_\mu^* + iC\,\epsilon^*\cdot q\,(p_B+p_{K^*})_\mu + iD\,\epsilon^*\cdot q\,q_\mu \right\} \\
&+ (\bar{u}(p_-)\gamma^\mu\gamma_5 v(p_+)) \times \\
&\qquad \left\{ -2F_1\epsilon_{\mu\nu\lambda\sigma}\epsilon^{*\nu} p_{K^*}^\lambda q^\sigma - iF\epsilon_\mu^* + iG\,\epsilon^*\cdot q\,(p_B+p_{K^*})_\mu + iH\,\epsilon^*\cdot q\,q_\mu \right\} \\
&+ iB_1(\bar{u}(p_-)v(p_+))\,\epsilon^*\cdot q \; + iB_2\;(\bar{u}(p_-)\gamma_5 v(p_+))\,\epsilon^*\cdot q \\
&+ 8C_{TE}\;(\bar{u}(p_-)\sigma_{\mu\nu}v(p_+))\;\left\{ -2T_1\epsilon^{*\mu}(p_B+p_{K^*})^\nu + B_3\epsilon^{*\mu}q^\nu - B_4\,\epsilon^*\cdot q\,p_{K^*}^\mu q^\nu \right\} \\
&+ 2iC_T\;\epsilon_{\mu\nu\lambda\sigma}\;(\bar{u}(p_-)\sigma^{\mu\nu}v(p_+))\;\left\{ -2T_1\epsilon^{*\lambda}(p_B+p_{K^*})^\sigma + B_3\epsilon^{*\lambda}q^\sigma - B_4\,\epsilon^*\cdot q\,p_{K^*}^\lambda q^\sigma \right\} \Bigg],
\end{aligned}
\tag{A.6}
$$

with the quantities $A, B, C, D, F_1, F, G, H,$ that are relevant for VA interactions, defined as

$$
\begin{aligned}
A &= 2(C_9^{eff} + R_V + R_V')\,\frac{V(q^2)}{m_B(1+\hat{k})} + \frac{4m_b C_7^{eff} T_1(q^2)}{q^2}\;, \\
B &= 2(C_9^{eff} + R_V - R_V')\,m_B(1+\hat{k})A_1(q^2) + 4m_b C_7^{eff}(1-\hat{k}^2)\,\frac{T_2(q^2)}{(q^2/m_B^2)}\;, \\
C &= 2(C_9^{eff} + R_V - R_V')\,\frac{A_2(q^2)}{m_B(1+\hat{k})} + \frac{4m_b C_7^{eff}}{q^2}\left[T_2(q^2) + \frac{(q^2/m_B^2)}{(1-\hat{k}^2)}\,T_3(q^2)\right]\;, \\
D &= \frac{4\hat{k}}{m_B}(C_9^{eff} + R_V - R_V')\,\frac{A_3(q^2)-A_0(q^2)}{(q^2/m_B^2)} - \frac{4m_b C_7^{eff} T_3(q^2)}{q^2}\;, \\
F_1 &= (C_{10} + R_A + R_A')\,\frac{2V(q^2)}{m_B(1+\hat{k})}\;, \\
F &= 2(C_{10} + R_A - R_A')\,m_B(1+\hat{k})A_1(q^2)\;, \\
G &= (C_{10} + R_A - R_A')\,\frac{2A_2(q^2)}{m_B(1+\hat{k})}\;, \\
H &= \frac{4\hat{k}}{m_B}(C_{10} + R_A - R_A')\,\frac{A_3(q^2)-A_0(q^2)}{(q^2/m_B^2)}\;.
\end{aligned}
\tag{A.7}
$$

The quantities $B_{1,2,3,4}$, relevant for SP and T interactions, are defined as

$$\begin{aligned}
B_1 &= -4(R_S - R'_S)\,\frac{\hat{k}}{(m_b/m_B)}\,A_0(q^2)\ , \\
B_2 &= -4(R_P - R'_P)\,\frac{\hat{k}}{(m_b/m_B)}\,A_0(q^2)\ , \\
B_3 &= 2(1-\hat{k}^2)\,\frac{T_1(q^2) - T_2(q^2)}{(q^2/m_B^2)}\ , \\
B_4 &= \frac{4}{q^2}\left(T_1(q^2) - T_2(q^2) - \frac{(q^2/m_B^2)}{(1-\hat{k}^2)}\,T_3(q^2)\right), \qquad \text{(A.8)}
\end{aligned}$$

where $q = (p_+ + p_-)$ and $\hat{k} \equiv m_{K^*}/m_B$.

The double differential decay rate is given by

$$\frac{d^2\Gamma}{dq^2 d\cos\theta} = \frac{1}{2E_B}\frac{2v\sqrt{\lambda}}{(8\pi)^3}|M|^2\ , \qquad \text{(A.9)}$$

where $v \equiv \sqrt{1-4m_l^2/q^2}$. Here $\lambda \equiv 1 + \hat{r}^2 + z^2 - 2(\hat{r}+z) - 2\hat{r}z$, with $\hat{r} \equiv m_{K^*}^2/m_B^2$ and $z \equiv q^2/m_B^2$. This leads to the differential branching ratio:

$$\frac{dB}{dq^2} = \frac{G^2\alpha^2}{2^{14}}\frac{1}{\pi^5}|V_{tb}V_{ts}^*|^2 m_B \tau_B \sqrt{\lambda}\,\Theta\ , \qquad \text{(A.10)}$$

where τ_B is the lifetime of B meson. The quantity Θ has the form

$$\Theta = \frac{1}{3\hat{r}}\Big[X_{SP} + X_{VA} + X_T + X_{SP\text{-}VA} + X_{SP\text{-}T} + X_{VA\text{-}T}\Big]\ , \qquad \text{(A.11)}$$

where the complete expressions for the X terms are:

$$\begin{aligned}
X_{SP} &= 3\,|B_1|^2\,m_B^2 z v^2 \lambda + 3\,|B_2|^2\,m_B^2 z\lambda \\
X_{VA} &= -8\,|A|^2\,m_B^4 \hat{r} z\left(v^2-3\right)\lambda - |B|^2\left(v^2-3\right)(12\hat{r}z+\lambda) - |C|^2\,m_B^4\left(v^2-3\right)\lambda^2 \\
&\quad + |F|^2\left(24\hat{r}zv^2 - \left(v^2-3\right)\lambda\right) + 16\,|F_1|^2\,m_B^4\hat{r}zv^2\lambda \\
&\quad + |G|^2\,m_B^4\lambda\Big(-6(\hat{r}+1)z\left(v^2-1\right) + 3z^2\left(v^2-1\right) - \left(v^2-3\right)\lambda\Big) \\
&\quad - 3\,|H|^2\,m_B^4 z^2\left(v^2-1\right)\lambda + 2\mathrm{Re}\left(FG^*\right)m_B^2\lambda\Big(-\hat{r}\left(v^2-3\right) + (2z+1)v^2 - 3\Big) \\
&\quad + 6\mathrm{Re}\left(FH^*\right)m_B^2 z\left(v^2-1\right)\lambda + 6\mathrm{Re}\left(GH^*\right)m_B^4(\hat{r}-1)z\left(v^2-1\right)\lambda \\
&\quad - 2\mathrm{Re}\left(BC^*\right)m_B^2\left(v^2-3\right)\lambda(\hat{r}+z-1)
\end{aligned}$$

$$
\begin{aligned}
X_T = 16m_B^2\,|C_{TE}|^2 \Bigg\{ & -4B_3^2 z\left(2v^2-3\right)(12\hat{r}z+\lambda) \\
& -4B_3 z\left(2v^2-3\right)\lambda\left(B_4 m_B^2(\hat{r}+z-1)+44T_1\right) \\
& -192B_3 zT_1\left(2v^2-3\right)\left(2\hat{r}z+\hat{r}-(z-1)^2\right)-B_4^2 m_B^4 z\left(2v^2-3\right)\lambda^2 \\
& -8T_1\lambda\left(B_4 m_B^2 z\left(2v^2-3\right)(3\hat{r}-z+1)+2T_1\left(8\hat{r}\left(v^2-3\right)+25z\left(2v^2-3\right)\right)\right) \\
& -192zT_1^2\left(2v^2-3\right)\left(3\hat{r}(z+2)-2(z-1)^2\right)\Bigg\} \\
& +4m_B^2\,|C_T|^2\Bigg\{4\lambda\Bigg(v^2\Bigg(2zT_1\left(22B_3+B_4 m_B^2(3\hat{r}-z+1)\right) \\
& +B_3 z\left(B_3+B_4 m_B^2(\hat{r}+z-1)\right)+4T_1^2(25z-8\hat{r})\Bigg)+96\hat{r}T_1^2\Bigg) \\
& +48zv^2\Bigg((B_3+2T_1)(B_3\hat{r}z+2T_1(z(3\hat{r}-2z+4)-2))+4\hat{r}T_1(B_3+6T_1)\Bigg) \\
& +B_4^2 m_B^4 z v^2\lambda^2\Bigg\} \\
X_{SP\text{-}VA} = {} & 12m_B\hat{m}_l\lambda\mathrm{Re}\left(B_2^* F\right)-12m_B^3\hat{m}_l(\hat{r}-1)\lambda\mathrm{Re}\left(B_2^* G\right)+12m_B^3\hat{m}_l z\lambda\mathrm{Re}\left(B_2^* H\right) \\
X_{SP\text{-}T} = {} & 0 \\
X_{VA\text{-}T} = {} & 768m_B^3\hat{m}_l\hat{r}T_1\lambda\mathrm{Re}\left(A^* C_T\right)+48m_B\hat{m}_l\mathrm{Re}\left(B^* C_{\mathrm{TE}}\right)\times \\
& \Bigg(2B_3(12\hat{r}z+\lambda)+B_4 m_B^2\lambda(\hat{r}+z-1)+T_1\left(96\hat{r}z+48\hat{r}-48z^2+96z+44\lambda-48\right)\Bigg) \\
& +48m_B^3\hat{m}_l\lambda\mathrm{Re}\left(C^* C_{TE}\right)\Bigg(2B_3(\hat{r}+z-1)+B_4 m_B^2\lambda+4T_1(3\hat{r}-z+1)\Bigg) \qquad \text{(A.12)}
\end{aligned}
$$

Note that here, we do not differentiate between the contributions from the SM and the new VA operators. The forward-backward asymmetry can also be written in the form

$$
A_{\mathrm{FB}}(q^2) = 2m_B\frac{\sqrt{\lambda}}{\hat{r}\Theta}\Big[Y_{SP}+Y_{VA}+Y_T+Y_{SP\text{-}VA}+Y_{SP\text{-}T}+Y_{VA\text{-}T}\Big]\,, \qquad \text{(A.13)}
$$

with the complete expressions for the Y terms given as

$$
\begin{aligned}
Y_{SP} &= 0\,, \\
Y_{VA} &= -4m_B\hat{r}z\mathrm{Re}\Big(A^* F+B^* F_1\Big)\,, \\
Y_T &= 0\,,
\end{aligned}
$$

$$
\begin{aligned}
Y_{SP\text{-}VA} &= \hat{m}_l(\hat{r}+z-1)\mathrm{Re}\left(B^*B_1\right) + m_B^2\hat{m}_l\lambda\mathrm{Re}\left(B_1^*C\right)\ , \\
Y_{SP\text{-}T} &= m_B z\mathrm{Re}(2B_1^*C_{TE}+B_2^*C_T)\Big(2B_3(\hat{r}+z-1)+B_4m_B^2\lambda+4T_1(3\hat{r}-z+1)\Big)\ , \\
Y_{VA\text{-}T} &= 2\mathrm{Re}\left(F^*C_T\right)\hat{m}_l\Big(2B_3(\hat{r}+z-1)+B_4m_B^2\lambda+T_1(44\hat{r}-4z+4)\Big) \\
&\quad -2\mathrm{Re}\left(G^*C_T\right)m_B^2\hat{m}_l\Big(2B_3\left(3\hat{r}z-z^2+z+\lambda\right)+B_4m_B^2(\hat{r}-1)\lambda \\
&\quad +4T_1\left(5\hat{r}z+4\hat{r}-3z^2+7z+3\lambda-4\right)\Big) \\
&\quad +2\mathrm{Re}\left(H^*C_T\right)m_B^2\hat{m}_l z\Big(2B_3(\hat{r}+z-1)+B_4m_B^2\lambda+4T_1(3\hat{r}-z+1)\Big) \\
&\quad -64\mathrm{Re}\left(F_1^*C_{TE}\right)m_B^2\hat{m}_l\Big(B_3\hat{r}z+2T_1\left(2\hat{r}z+\hat{r}-(z-1)^2+\lambda\right)\Big)\ . \qquad \text{(A.14)}
\end{aligned}
$$

References

[1] H. Y. Cheng, C. K. Chua and A. Soni, *Phys. Rev.* **D 72** (2005) 094003 [hep-ph/0506268]; G. Buchalla, G. Hiller, Y. Nir and G. Raz, *J. High Energy Phys.* **0509** (2005) 074 [hep-ph/0503151]; E. Lunghi and A. Soni, *J. High Energy Phys.* **0908** (2009) 051 [arXiv:0903.5059 [hep-ph]].

[2] In the latest update of the πK puzzle, it was seen that, although NP was hinted at in $B \to \pi K$ decays, it could be argued that the SM can explain the data, see S. Baek, C. W. Chiang and D. London, *Phys. Lett.* **B 675** (2009) 59.

[3] E. Barberio *et al.* [Heavy Flavor Averaging Group], hep-ex/0808.1297; M. Bona *et al.* [UTfit Collaboration], arXiv:0803.0659 [hep-ph].

[4] T. Feldmann and J. Matias, *J. High Energy Phys.* **0301** (2003) 074 [hep-ph/0212158]; B. Aubert *et al.* [BABAR Collaboration], *Phys. Rev. Lett.* **102** (2009) 091803 [arXiv:0807.4119 [hep-ex]].

[5] A. Ishikawa *et al.*, *Phys. Rev. Lett.* **96** (2006) 251801 [hep-ex/0603018]; J. T. Wei *et al.* [BELLE Collaboration], *Phys. Rev. Lett.* **103** (2009) 171801 [arXiv:0904.0770 [hep-ex]].

[6] B. Aubert *et al.* [BABAR Collaboration], *Phys. Rev.* **D 73** (2006) 092001 [hep-ex/0604007], *Phys. Rev.* **D 79** (2009) 031102 [arXiv:0804.4412 [hep-ex]].

[7] W. Altmannshofer, P. Ball, A. Bharucha, A. J. Buras, D. M. Straub and M. Wick, *J. High Energy Phys.* **0901** (2009) 019 [arXiv:0811.1214 [hep-ex]].

[8] G. Burdman, *Phys. Rev.* **D 57** (1998) 4254 [hep-ph/9710550]; A. Ali, P. Ball, L. T. Handoko and G. Hiller, *Phys. Rev.* **D 61** (2000) 074024 [hep-ph/9910221].

[9] M. Beneke, T. Feldmann and D. Seidel, *Nucl. Phys.* **B 612** (2001) 25 [hep-ph/0106067].

[10] "Belle Finds a Hint of New Physics in Extremely Rare B Decays" reported in August 2009 (as Press Release): http://www.kek.jp/intra-e/press/2009/BellePress14e.html.

[11] An early study of new physics and $A_{\rm FB}$ in $\bar{B} \to \bar{K}^* \mu^+ \mu^-$ can be found in A. S. Cornell, N. Gaur and S. K. Singh, hep-ph/0505136.

[12] See, for example, A. Ali, T. Mannel and T. Morozumi, *Phys. Lett.* **B 273** (1991) 505; A. J. Buras and M. Munz, *Phys. Rev.* **D 52** (1995) 186 [hep-ph/9501281]. M. Misiak, *Nucl. Phys.* **B 393** (1993) 23 [Erratum-ibid. B **439**, 461 (1995)]; A. Ali, P. Ball, L. T. Handoko and G. Hiller, Ref. [8]; F. Kruger and E. Lunghi, *Phys. Rev.* **D 63** (2001) 014013 [hep-ph/0008210]; A. Ali, E. Lunghi, C. Greub and G. Hiller, *Phys. Rev.* **D 66** (2002) 034002 [hep-ph/0112300]; A. Ghinculov, T. Hurth, G. Isidori and Y. P. Yao, *Eur. Phys. J.* **C 33** (2004) S288 [hep-ph/0310187]; W. Altmannshofer et al., Ref. [7].

[13] See, for example, C. Bobeth, T. Ewerth, F. Kruger and J. Urban, *Phys. Rev.* **D 64** (2001) 074014 [hep-ph/0104284]; P. H. Chankowski and L. Slawianowska, *Eur. Phys. J.* **C 33** (2004) 123 [hep-ph/0308032]; G. Hiller and F. Kruger, *Phys. Rev.* **D 69** (2004) 074020 [hep-ph/0310219]; A. K. Alok and S. U. Sankar, *Phys. Lett.* **B 620** (2005) 61 [hep-ph/0502120]; A. K. Alok, A. Dighe and S. U. Sankar, [arXiv:0803.3511 [hep-ph]], *Phys. Rev.* **D 78** (2008) 034020 [arXiv:0805.0354 [hep-ph]]; W. Altmannshofer et al., Ref. [7].

[14] A. Hovhannisyan, W. S. Hou and N. Mahajan, *Phys. Rev.* **D 77** (2008) 014016 [hep-ph/0701046].

[15] F. Kruger and J. Matias, *Phys. Rev.* **D 71** (2005) 094009 [hep-ph/0502060].

[16] E. Lunghi and J. Matias, *J. High Energy Phys.* **0704** (2007) 058 [hep-ph/0612166].

[17] U. Egede, T. Hurth, J. Matias, M. Ramon and W. Reece, *J. High Energy Phys.* **0811** (2008) 032 [arXiv:0807.2589 [hep-ph]].

[18] T. M. Aliev, V. Bashiry and M. Savci, *Eur. Phys. J.* **C 35** (2004) 197 [hep-ph/0311294], *J. High Energy Phys.* **0405** (2004) 037 [hep-ph/0403282]; T. M. Aliev, M. K. Cakmak, A. Ozpineci and M. Savci, *Phys. Rev.* **D 64** (2001) 055007 [hep-ph/0103039]; W. Bensalem, D. London, N. Sinha and R. Sinha, *Phys. Rev.* **D 67** (2003) 034007 [hep-ph/0209228].

[19] Mitesh Patel, private communication.

[20] A. K. Alok, A. Dighe and S. Uma Sankar, *Phys. Rev.* **D 78** (2008) 114025 [arXiv:0810.3779 [hep-ph]].

[21] C. Bobeth, M. Misiak and J. Urban, *Nucl. Phys.* **B 574** (2000) 291 [hep-ph/9910220].

[22] A. Ali, P. Ball, L. T. Handoko and G. Hiller, Ref. [8].

[23] A. J. Buras and M. Munz, Ref. [12].

[24] Y. Nir, *Phys. Lett.* **B 221** (1989) 184.

[25] M. Iwasaki *et al.* [Belle Collaboration], `hep-ex/0503044`.

[26] B. Aubert *et al.* [BABAR Collaboration], *Phys. Rev. Lett.* **93** (2004) 081802 [`hep-ex/0404006`].

[27] T. Huber, T. Hurth and E. Lunghi, *Nucl. Phys.* **B 802** (2008) 40 [`arXiv:0712.3009` [hep-ph]].

[28] M. Blanke, A. J. Buras, D. Guadagnoli and C. Tarantino, *J. High Energy Phys.* **0610** (2006) 003 [`hep-ph/0604057`].

[29] T. Aaltonen *et al.* [CDF Collaboration], *Phys. Rev. Lett.* **100** (2008) 101802 [`arXiv:0712.1708` [hep-ph]].

[30] C. Amsler *et al.* [Particle Data Group], *Phys. Lett.* **B 667** (2008) 1.

[31] C. Aubin, `arXiv:0909.2686` [hep-lat].

[32] S. Fukae, C. S. Kim, T. Morozumi and T. Yoshikawa, *Phys. Rev.* **D 59** (1999) 074013 [`hep-ph/9807254`].

[33] T. M. Aliev, C. S. Kim and Y. G. Kim, *Phys. Rev.* **D 62** (2000) 014026 [`hep-ph/9910501`].

[34] J. Charles, A. Le Yaouanc, L. Oliver, O. Pene and J. C. Raynal, *Phys. Rev.* **D 60** (1999) 014001 [`hep-ph/9812358`].

[35] J. Charles, A. Le Yaouanc, L. Oliver, O. Pene and J. C. Raynal, *Phys. Lett.* **B 451** (1999) 187 [`hep-ph/9901378`].

[36] M. J. Dugan and B. Grinstein, *Phys. Lett.* **B 255** (1991) 583.

[37] M. Beneke and T. Feldmann, *Nucl. Phys.* **B 592** (2001) 3 [`hep-ph/0008255`].

[38] C. W. Chiang, R. H. Li and C. D. Lu, `arXiv:0911.2399` [hep-ph].

[39] C. Bobeth, G. Hiller and G. Piranishvili, *J. High Energy Phys.* **0712** (2007) 040 [`arXiv:0709.4174` [hep-ph]].

[40] S. Davidson, D. C. Bailey and B. A. Campbell, *Z. Physik* **C 61** (1994) 613 [`hep-ph/9309310`]; M. Hirsch, H. V. Klapdor-Kleingrothaus and S. G. Kovalenko, *Phys. Lett.* **B 378** (1996) 17 [`hep-ph/9602305`].

[41] P. Gambino, U. Haisch and M. Misiak, *Phys. Rev. Lett.* **94** (2005) 061803 [`hep-ph/0410155`].